Ecological Modelling 488 (2024) 110575

Contents lists available at ScienceDirect

Ecological Modelling

journal homepage: www.elsevier.com/locate/ecolmodel

Development and application of a bioenergetics growth model for multiple early life stages of an ecologically important marine fish

Mark M. Morales [a,*], Jerome Fiechter [b], John C. Field [c,d], Neosha S Kashef [c,d], Elliott L. Hazen [a,e,f], Mark H. Carr [a]

[a] Department of Ecology and Evolutionary Biology, University of California, Santa Cruz, Santa Cruz, CA, United States
[b] Department of Ocean Sciences, University of California, Santa Cruz, Santa Cruz, CA, United States
[c] Fisheries Ecology Division, Southwest Fisheries Science Center, National Marine Fisheries Service, National Oceanic and Atmospheric Administration, Santa Cruz, California, USA
[d] Fisheries Collaborative Program, Institute of Marine Sciences, University of California, Santa Cruz, Santa Cruz, California, USA
[e] Environmental Research Division, NOAA Southwest Fisheries Science Center, Monterey, CA, USA
[f] Hopkins Marine Station, Department of Biology, Stanford University, Pacific Grove, CA, USA

ARTICLE INFO

Keywords:
Physical-biogeochemical model
Larval growth
Rockfish biology
Ocean temperature
Food availability
Bioenergetics

ABSTRACT

Spatial and temporal variability in temperature and food availability are key drivers of growth of marine fishes. Growth during the early life stages (ELS's) is tightly coupled to survival, and in turn, can set year-class strength (i.e. annual recruitment) and overall stock productivity of populations and fished stocks. Ontogenetic changes in physiology, dietary preferences, and growth across ELS's can be accounted for within bioenergetics models, but existing models lack resolution within larval and early juvenile stages. We leveraged daily output from a coupled physical-biogeochemical model to force a highly resolved ontogenetic bioenergetics model parametrized for an ecologically important rockfish in the California Current System. Size-at-age predictions closely track empirical growth trajectories of the ELS's. Scenario testing revealed that growth performance is disproportionately driven by changes in temperature compared to food availability. We then expanded the model to incorporate spatial climatological differences in temperature and prey concentration and found that preflexion growth potential is maximized in areas of historical spawning, suggesting the timing and location of reproduction is an adaptive strategy that places larvae in habitat favorable for survival. Growth potential for late-stage larvae (postflexion) is greatest over a broad areal extent, implying that if a particle tracking algorithm was coupled to the bioenergetics model, a wide range of larval dispersal pathways would place postflexion larvae in habitat suitable for rapid growth. Finally, growth potential of pelagic juveniles is maximized over the continental shelf and shelf-break, aligning with high juvenile catch rates from a fisheries-independent survey. In summary, this study (i) serves as a proof of concept that a bioenergetics model with high ontogenetic resolution can reproduce life stage-specific growth trajectories even though the underlying physiology data for model parameterization is imperfect and (ii) can aid future studies aimed at understanding how ecosystem processes interact with ontogenetic growth and changes in year class strength of early life stages of marine fishes.

1. Introduction

Temperature and food availability are key drivers of the rate of somatic growth of marine ectotherms (Winberg, 1956). Since body size is intimately linked with survival (Pepin, 1991; Sogard, 1997) and fecundity (Hixon et al., 2014; Dick et al., 2017), processes directly affecting the growth and condition of an individual contribute to their susceptibility to starvation and predation risk (Bailey and Houde, 1989; Houde, 1987), and influence reproductive output. Hence, characterizing growth rate variability is important for understanding the dynamics of fish populations alongside the communities and ecosystems that depend on them. For marine ectotherms, such as bony fishes, metabolic rates are dependent on body size (Brown et al., 2004), ambient (seawater) temperature (Fry 1971), oxygen concentration (Yang et al., 1992), and seawater pH (Hamilton et al., 2017). Marine fishes are adapted to a thermal range at which physiological function is optimized (Pörtner and

* Corresponding author.
E-mail address: morales.760.mark@gmail.com (M.M. Morales).

https://doi.org/10.1016/j.ecolmodel.2023.110575
Received 18 August 2023; Received in revised form 20 November 2023; Accepted 23 November 2023
Available online 14 December 2023

Farrel 2008). When water temperature exceeds the optima, growth rates can increase if increased prey availability can offset elevated metabolic rates (Munday et al., 2009). If adequate food is not available to offset increased maintenance costs, individuals will suffer greater mortality and populations can decline (Pörtner and Knust, 2007).

For the early life stages (ELS) of fishes, energy reserves are limited due to their small size and higher mass-specific metabolic rates (Peck and Moyano, 2016), ultimately putting them at higher risk of starvation relative to adult conspecifics. In the face of expected global change, increasing water temperatures are predicted to decrease developmental time and shorten pelagic larval durations (O'Connor *et al.*, 2007), affecting population connectivity, genetic diversity, trophic interactions and population dynamics. Furthermore, since year-class strength (recruitment) is believed to be set primarily during early developmental stages (Hjort, 1914; Houde, 2016), there is a need to perform mechanistic studies of growth rate variability through use of energetic models in relation to natural climate variability, anthropogenic environmental change, and population productivity (Hollowed et al., 2011).

Energy budget modeling is a method used to assess the amalgamation of consumption, metabolism, somatic growth, excretion, and reproduction and how temperature and food availability interact with these rates (Chipps and Wahl, 2008). Bioenergetic models are grounded by the first law of thermodynamics where energy consumed is balanced by energy used for metabolism, excretion of waste products, and somatic and gonadal growth (Winberg 1956). Three modeling frameworks are commonly used in fish bioenergetics: (i) the metabolic theory of ecology (Brown et al., 2004), (ii) dynamic energy budget (DEB; Kooijman, 2010), and (iii) the "Wisconsin model" (Kitchell et al, 1977; Sibly et al., 2013; Jørgensen et al., 2016). The Wisconsin model is a frequently used framework, primarily because of the development of accessible and computationally efficient software (Hewett and Johnson 1987, 1992; Hanson et al. 1997; Deslauriers et al., 2017).

Historically, bioenergetics models were forced by point source measurements of temperature to quantify the proportion of maximum consumption required to achieve observed growth rates (Kitchell et al., 1977). However, Rose et al., (1999a and 1999b) developed a consumption term based on a multispecies Holling's Type II functional response that allowed for the estimation of consumption rates given dietary preferences and variable prey densities. Until recently, measurements of food availability used to force the feeding module relied on sparse and infrequently sampled in situ prey concentrations, which suffer from insufficiencies due to high levels of variability within and among sampling sites (Young et al., 2009). Coupled physical-biogeochemical models allow bioenergetics modelers to circumvent the use of 'snapshot' empirical prey availabilities with fine-scale spatiotemporal temperature and prey fields (Ito et al., 2004; Megrey et al., 2007). Furthermore, ontogenetic changes in consumption, or growth, within larval development stages are not typically accounted for in bioenergetics models, despite the recognition that somatic growth varies across ELS's (Laidig et al., 1991) and the directionality of growth-dependent mortality can vary depending on developmental stage (Bailey and Houde, 1989; Houde, 1997). The lack of highly resolved ontogenetic bionenergetics models for ELS fishes is primarily due to a paucity of life stage-specific estimates of allometric respiration and consumption measurements, which are difficult to accurately measure in controlled laboratory settings (Peck and Moyano, 2016). However, accounting for ontogenetic differences in growth within a bioenergetics framework could possibly be achieved if life stage-specific dietary preferences based off larval and juvenile feeding habit studies are available. In addition, stage-specific feeding rate parameters within the realized consumption term (Rose et al., 1999a; 1999b) could be calibrated by minimizing the deviance between predicted growth and empirical growth curves that account for ontogenetic growth differences in the ELS. Development of a model that accounts for fine-scale ontogenetic changes of ELS growth could help identify the conditions and early life history stage that is most important for setting year-class strength under the growth-dependent mortality paradigm (Anderson 1988; Miller et al.,1988). For example, there is evidence that juvenile quillback rockfish (*Sebastes maliger*) experience size-selective predation mortality, with smaller, slower growing individuals occurring more frequently in juvenile coho salmon stomachs (*Onorhynchus kisutch*), suggesting growth could be an important driver of survival for rockfish (Fennie et al., 2020).

Rockfishes (Sebastes spp.) are a highly speciose family of fishes in the California Current System (CCS) with ecological and economic importance. Rockfishes are viviparous, giving birth to live, ready-to-feed larvae (~5 mm standard length; SL) primarily during the winter and spring months (Love et al., 2002). Of the nearly 70 species of rockfish in the CCS, shortbelly rockfish (Sebastes jordani) are among the most abundant, comprising ~50% of juvenile rockfish catch in midwater trawls (Field et al., 2021), with the top ten species of rockfish caught in central California covarying in abundance (Ralston et al., 2013). The ELS of rockfishes display large interannual variation in survivorship as revealed through larval abundance (Thompson et al. 2016,2017), pelagic juvenile abundance (Ralston et al., 2013; Santora et al., 2017; Schroeder et al., 2014; 2019) and recruitment estimates from stock assessments (PFMC https://www.pcouncil.org/). There is now a substantial body of evidence suggesting a linkage between environmental conditions during ELS and the strength of recruitment of rockfishes (Woodbury and Ralston, 1991; Ainley et al., 1993; Ralston and Howard, 1995; Laidig et al., 2007; Laidig, 2010; Caselle et al., 2010; Ralston et al., 2013; Schroeder et al., 2014; 2019; Friedman et al., 2018). Dietary studies reveal that larval and juvenile rockfishes preferentially feed on copepods and krill, respectively (Sumida and Moser, 1984; Reilly et al., 1992; Shaffer et al., 1995; Miller and Broduer, 2007; Miller et al., 2010; Bosley et al., 2014), whose abundances are forced by interannual changes in climatic conditions (Rebstock, 2001; Bi et al., 2011; Santora et al., 2014). Variability in growth and survival of larval and juvenile rockfishes in relation to temperature variability and food availability has not been conducted beyond correlational studies (e.g. Peterson et al., 2014). Mechanistic models grounded in first principles (i.e. physiology) are the next step in understanding the relationship between temperature, prey abundance and growth of ELS rockfishes.

Here we develop a novel ELS bioenergetics model that accounts for changes in growth rate (i.e., stanzas) across three larval stages (preflexion, flexion, and postflexion) and the pelagic juvenile stage for an ecologically important marine fish, the shortbelly rockfish (*Sebastes jordani*). Life stage transitions in the model (governed by changes in consumption parameters) are assumed to be deterministic and based off length alone, rather than morphological development which is not accounted for in bioenergetics models. Specifically, we parameterize the bioenergetic model and compare predictions to an empirical growth curve with high ontogenetic resolution, assess the behavior of the model through sensitivity analysis, and explore the relative influence of temperature and prey availability on growth through scenario testing. Then we apply the model to a 2-D Eulerian application to investigate ELS-specific spatial patterns of growth potential in relation to spawning locations and settlement sites by forcing it with temperature and prey concentration from an existing high resolution coupled physical-biogeochemical historical simulation for the central California Current region. This work acts as a proof concept that within-ELS growth stanzas can be modeled accurately using imperfect physiological parameterizations given sufficient ecological data. Further, the model can be extended for use in Lagrangian individual-based models to better understand the influence of biophysical interactions on within-ELS growth differences and to evaluate mechanisms of recruitment, the 'holy grail' of fisheries oceanography.

2. Methods

2.1. Coupled Physical-Biogeochemical Historical Simulation

Temperature and food availability are required inputs to bioenergetically model temporal changes in somatic growth of marine fishes. Since empirical observations of subsurface temperatures and prey fields in general are sparse and inconsistent, we rely here on output from an existing coupled physical-biogeochemical historical simulation for 1988-2010 (Fiechter et al., 2018; Fiechter et al., 2020). Briefly, the physical-biogeochemical model is a nested implementation of the Regional Ocean Modeling System (ROMS) (Shchepetkin et al., 2005; Haidvogel et al., 2008) at 3 km horizontal resolution, coupled to a customized biogeochemical model (NEMUCSC) adapted from the North Pacific Ecosystem Model for Understanding Regional Oceanography (NEMURO) of Kishi et al. (2007) and including two phytoplankton functional groups (nanophytoplankton and diatoms) and three zooplankton size classes (small, large, and predatory). The nested ROMS-NEMUCSC historical simulation for the central CCS has been used to examine variability in alongshore coastal upwelling intensity and primary production (Fiechter et al., 2018), phenology and drivers of krill aggregations (Fiechter et al., 2020), and spatiotemporal patterns of coastal ocean acidification and hypoxia (Cheresh and Fiechter, 2020; 2023). The historical simulation has also been evaluated for its capability to reproduce temperature, salinity and density variability adequately in the central CCS (Schroeder et al. 2014; 2019).

Daily mean values of temperature, small zooplankton (ZS), large zooplankton (ZL) and predatory zooplankton (ZP) from ROMS-NEMUCSC were calculated over the period 1988-2010 to produce a climatology of temperature and three prey concentrations. For spatially invariant simulations (0-D) of the bioenergetics model, these variables were spatially averaged over coastal central California (36°- 39°N; 124°-121.5°W; Fig. 1) to calibrate simulated growth trajectories of ELS rockfish with empirical growth from the same area (see 2.4 Simulations). We selected temperature, ZS, ZL, and ZP at 30m depth as this is where the ELS of shelf and shelf-slope rockfishes are most abundant (Moser and Boehlert, 1991; Ross and Larson, 2003) and is the target depth of midwater pelagic trawl data used for model evaluation (Sakuma et al., 2016; Field et al. 2021).

2.2. Bioenergetics Model

Somatic growth of an individual is calculated daily as the difference between consumption and the sum of respiration, specific dynamic action, egestion and excretion. The formulation and terminology for the bioenergetics model follow that of the Wisconsin Bioenergetics model (Kitchell et al., 1977; Hewett and Johnson, 1987; 1992; Hanson et al., 1997; Deslauriers et al., 2017), with adaptations to account for variable food availability (Rose et al., 1999a; 1999b). The somatic growth rate of an individual is given by:

$$\frac{dW}{dt} = [C - (R + SDA + EG + EX)] \cdot W \cdot \frac{ED_{zoopl}}{ED_{fish}} \tag{1}$$

where W is the wet weight (g fish) of an individual at time t (d) . C is consumption, R is respiration or losses through metabolism, SDA is the specific dynamic action or costs to digestion, EG is egestion, EX is excretion, ED_{fish} is the energy density of ELS rockfish (Joules · g fish^{-1}), and ED_{zoopl} is the energy density of zooplankton (Joules · g prey^{-1}). The units of consumption, respiration, specific dynamic action, egestion and excretion are in g prey · g fish^{-1} · d^{-1}, which are converted to g fish · g fish^{-1} · d^{-1} through the ratio of the energy density of zooplankton (ED_{zoopl}) relative to the energy density of fish (ED_{fish}), which we assume are constant following Megrey et al. (2007) for simplicity. Parameter values and their sources are provided in Table 1.

2.2.1. Consumption

Daily consumption rate (g prey · g fish^{-1} · d^{-1}) is calculated as the percentage of maximum consumption, offset by a temperature-dependent scaling factor:

$$C_{max} = a_C \cdot W^{b_C} \cdot F_C(T) \tag{2}$$

where C_{max} is maximum consumption rate (g prey · g fish^{-1} · d^{-1}), a_C is the intercept for the allometric mass function, W is the wet weight (g) of ELS rockfish, b_C is the allometric slope, T is temperature, and $F_C(T)$ is the temperature-dependence function. Previous bioenergetics models of rockfishes were largely focused on settled juvenile or adult life history stages (Harvey et al., 2011; Rooper et al., 2012), and did not estimate growth given allometric consumption. Therefore, we derived a_C and b_C from Boehlert and Yoklavich (1983) (Table 1), who evaluated the effects of temperature, ration, and fish size upon growth for rockfish in the pelagic juvenile life history stage.

A dome-shaped temperature-dependence function is preferred over other functions when modeling effects of temperature on consumption for temperate fish species (Thornton and Lessem, 1978). Here we model the influence of temperature on maximum consumption as the product of two sigmoidal curves with one curve describing an increase in consumption with increasing temperature (*gcta*) and the other a decrease in

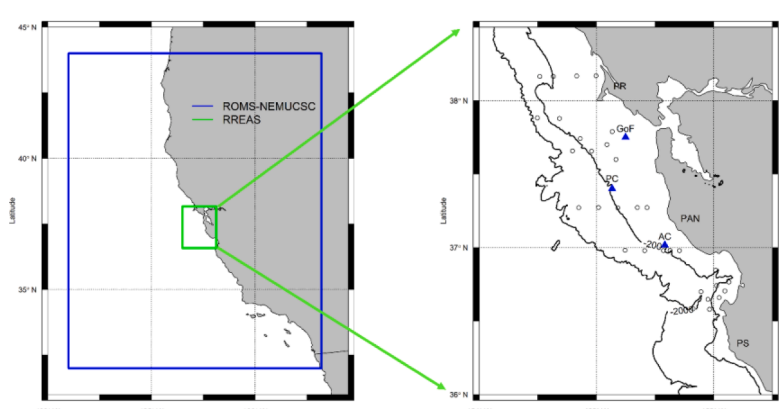

Fig. 1. Map of the California Current System and focal study area (inset). Spatial extents for the 3km resolution ROMS-NEMUCSC (blue box) and the core Rockfish Recruitment and Ecosystem Assessment Survey (RREAS) survey area (green box and inset). Spatial extent used for generating the 0-D climatology temperature and zooplankton concentrations from ROMS-NEMUCSC with RREAS sampling stations (open circles) and 200m and 2,000m isobaths shown. (inset) Major promontories are labeled on land (PR = Point Reyes; PAN = Point Año Nuevo; PS = Point Sur) and the Gulf of Farallones (GoF) and two canyon systems (blue diamond: PC = Pioneer Canyon; AC = Ascension Canyon) important to shortbelly rockfish (*Sebastes jordani*) life history.

Table 1
Summary of parameter values used in the shortbelly rockfish (*Sebastes jordani*) bioenergetics model.

Parameter	Description	Units	Value	Source
	Consumption			
a_C	Intercept for C_{max} at (te1+te3)/2	-	0.4613	Boehlert & Yoklavich, 1983
b_C	Coefficient for C_{max} vs. weight	-	-0.335	Boehlert & Yoklavich, 1983
te1	Temperature for xk1	°C	5	Derived
te2	Temperature for xk2	°C	8	Derived
te3	Temperature for xk3	°C	12	Derived
te4	Temperature for xk4	°C	20	Derived
xk1	Proportion of C_{max} at te1	-	0.1	Megrey et al., 2007
xk2	Proportion of C_{max} at te2	-	0.98	Megrey et al., 2007
xk3	Proportion of C_{max} at te3	-	0.98	Megrey et al., 2007
xk4	Proportion of C_{max} at te4	-	0.1	Megrey et al., 2007
	Multispecies functional response			
υ_{11}	Vulnerability of ZS to preflexion larvae	-	1	Sumida & Moser 1984
υ_{12}	Vulnerability of ZS to flexion larvae	-	0.5	Sumida & Moser 1984
υ_{13}	Vulnerability of ZS to postflexion larvae	-	0.5	Sumida & Moser 1984; Reilly et al., 1992
υ_{14}	Vulnerability of ZS to pelagic juveniles	-	0.2	Reilly et al., 1992
υ_{21}	Vulnerability of ZL to preflexion larvae	-	0	Sumida & Moser 1984
υ_{22}	Vulnerability of ZL to flexion larvae	-	0.5	Sumida & Moser 1984
υ_{23}	Vulnerability of ZL to postflexion larvae	-	0.5	Sumida & Moser 1984; Reilly et al., 1992
υ_{24}	Vulnerability of ZL to pelagic juveniles	-	0.3	Reilly et al., 1992
υ_{31}	Vulnerability of ZP to preflexion larvae	-	0	Sumida & Moser 1984
υ_{32}	Vulnerability of ZP to flexion larvae	-	0	Sumida & Moser 1984
υ_{33}	Vulnerability of ZP to postflexion larvae	-	0	Sumida & Moser 1984; Reilly et al., 1992
υ_{34}	Vulnerability of ZP to pelagic juveniles	-	0.5	Reilly et al., 1992
K_{11}	Half saturation constant for ZS to preflexion larvae	g fish wet weight m^{-3}	2	Calibrated
K_{12}	Half saturation constant for ZS to flexion larvae	g fish wet weight m^{-3}	1.5	Calibrated
K_{13}	Half saturation constant for ZS to postflexion larvae	g fish wet weight m^{-3}	0.5	Calibrated
K_{14}	Half saturation constant for ZS to pelagic juveniles	g fish wet weight m^{-3}	0.2	Calibrated
K_{21}	Half saturation constant for ZL to preflexion larvae	g fish wet weight m^{-3}	0	Calibrated
K_{22}	Half saturation constant for ZL to flexion larvae	g fish wet weight m^{-3}	1.4	Calibrated
K_{23}	Half saturation constant for ZL to postflexion larvae	g fish wet weight m^{-3}	0.5	Calibrated
K_{24}	Half saturation constant for ZL to pelagic juveniles	g fish wet weight m^{-3}	0.4	Calibrated
K_{31}	Half saturation constant for ZP to preflexion larvae	g fish wet weight m^{-3}	0	Calibrated
K_{32}	Half saturation constant for ZP to flexion larvae	g fish wet weight m^{-3}	0	Calibrated
K_{33}	Half saturation constant for ZP to postflexion larvae	g fish wet weight m^{-3}	0	Calibrated
K_{34}	Half saturation constant for ZP to pelagic juveniles	g fish wet weight m^{-3}	0.4	Calibrated
	Respiration			
a_R	Intercept for R	-	0.0143	Harvey et al., 2011; Rooper et al., 2012
a_C	Coefficient for R vs. weight	-	-0.2385	Harvey et al., 2011; Rooper et al., 2012
RQ	Slope for temperture dependence of respiration (Q10)	-	2	Harvey et al., 2011; Rooper et al., 2012
RTO	Optimum temperature for respiration	°C	23	Harvey et al., 2011; Rooper et al., 2012
RTM	Maximum temperature for respiration	°C	28	Harvey et al., 2011; Rooper et al., 2012
ACT	Activity Multiplier	-	1[a]; 1.8[b]; 1.7[c]; 1.6[d]	Rose et al., 2015
	Egestion and Excretion (Eg and U)			
a_F	Proportion of consumed food egested	-	0.104	Harvey et al., 2011; Rooper et al., 2012
a_E	Proportion of consumed food excreted	-	0.068	Harvey et al., 2011; Rooper et al., 2012
	Specific Dynamic Action			
SDA	Specific Dynamic Action	-	0.163	Harvey et al., 2011; Rooper et al., 2012
	Energy Density			
ED_{zoopl}	Energy density of zooplankton	J g $prey^{-1}$	2580	Megrey et al., 2007
ED_{fish}	Energy density of rockfish	J g $fish^{-1}$	4850	Spear, 1993; Warzybok et al., 2018

consumption with increasing temperature (*gctb*; Ito et al., 2004).

$$F_C(T) = gcta \cdot gctb, \tag{3}$$

where T is seawater temperature (°C) and gcta is calculated as

$$gcta = \frac{xk1 \cdot t4}{(1 + xk1) \cdot (t4 - 1)}, \tag{4}$$

$$t4 = e^{t5 \cdot (T - te1)}, \tag{5}$$

$$t5 = tt5 * ln\left(\frac{xk2 \cdot (1 - xk1)}{xk1 \cdot (1 - xk2)}\right), \tag{6}$$

$$tt5 = \frac{1}{te2 - te1}, \tag{7}$$

and gctb is calculated as

$$gctb = \frac{xk4 \cdot t6}{(1 + xk4) \cdot (t6 - 1)}, \tag{8}$$

$$t6 = e^{t7 \cdot (te4 - T)}, \tag{10}$$

$$t7 = tt7 \cdot ln\left(\frac{xk3 \cdot (1 - xk1)}{xk4 \cdot (1 - xk3)}\right), \tag{11}$$

$$tt7 = \frac{1}{te4 - te3}. \tag{12}$$

This formulation requires four parameters for seawater temperatures (i.e. te1, te2, te3, and te4) and four percentages of maximum consumption associated with each temperature (i.e. xk1, xk2, xk3, and xk4). Parameter te1 (te4) is the lower (higher) temperature at which temperature dependence is a small fraction (xk1 or xk4) of the maximum rate. Parameter te2 (te3) describes the peak of the ascending (descending) limb, set at xk2 and xk3, and can be thought of as the lower (upper) bound of the optimal temperature for consumption. Detailed experimental investigations of the effects of temperature on consumption of ELS rockfishes have not been conducted, therefore we assume that optimal thermal habitat occurs where ELS shortbelly rockfish (*Sebastes jordani*) are most commonly found in the central California Current. To that end, we plotted the frequency of positive catches of pelagic juvenile shortbelly relative to seawater temperature at 20-40m to find te2 and te3 in Equation 7 and 12, respectively (Figure S1). Pelagic juvenile data are from the Rockfish Recruitment and Ecosystem Assessment Survey (RREAS; see section 2.3). The lower (te1) and upper (te4) temperature thresholds were assumed to be 5°C and 20°C, which are generally outside the range of observed temperatures for the central CCS for the depth of ELS shortbelly rockfish (~30m; Moser and Boehlert, 1991).

To offset maximum consumption relative to the amount of prey available, we employed a variation of the Holling's type II functional response that accounts for multiple prey types (Rose et al., 1999a; 1999b) to calculate the realized daily consumption rate (C_{rel}) for each life stage i (C_i; g prey · g fish^{-1} · d^{-1}) by summing consumption across each prey type j:

$$C_{rel_i} = \sum_{j=1}^{3} C_{rel_{ij}}, \tag{13}$$

$$C_{rel_{ij}} = \frac{C_{max} \cdot \frac{PD_{ij} v_{ij}}{K_{ij}}}{1 + \sum_{k=1}^{3} \frac{PD_{ik} v_{ik}}{K_{ik}}}, \tag{14}$$

where C_{max} is the maximum consumption rate (g prey · g fish^{-1} · d^{-1}) of an individual of stage i, PD_{ij} is the density of prey type j (g prey · m^{-3}) for life stage i, v_{ij} is the vulnerability of prey type j (dimensionless) for life stage i, and K_{ij} is the half saturation constant (g prey · m^{-3}) for life stage i of prey type j. Given ontogenetic dietary preferences of ELS shortbelly (Sumida and Moser, 1984; Reilly et al., 1992), we use three prey types produced by NEMUCSC for prey density; small zooplankton (ZS; micrograzers; j=1), large zooplankton (ZL; copepods; j = 2), and predatory zooplankton (ZP; Euphausiids or krill; j = 3). Prey composition of preflexion larvae (standard length (SL) < 8 mm) is comprised mainly of calanoid copepod nauplii (~ 75%) and copepodites (~2-12%), with the relative contribution of copepodites being largest at flexion (~25%) after which adult copepods dominate (>40%) throughout the postflexion stage (SL < 30mm; Sumida and Moser, 1984; Reilly et al., 1992). Various stages of Euphausiids comprise ~50% of pelagic juvenile diet, with considerable contribution of copepods (Reilly et al., 1992). Vulnerability values (v_{ik}) were assigned using these dietary preferences (Table 1). NEMUCSC treats the three zooplankton groups as functional groups based on prey size with ZL and ZP representing copepods and Euphausiids, respectively. The units of prey densities in NEMUCSC are tracked in mol N l^{-1} and were converted to g · prey · m^{-3} by:

$$\frac{14\ g\ N}{mol\ N} \cdot \frac{1\ g\ dry\ weight}{0.07\ g\ N\ dry\ weight} \cdot \frac{1\ g\ wet\ weight}{0.2\ g\ dry\ weight} \cdot \frac{10^3 l}{m^3} = 10^{-6} g\ prey\ wet\ weight\ m^3. \tag{15}$$

Half-saturation coefficients, K_{ij}, are used as a factor to scale satiation and represent the PD_{ij} at which half of maximum consumption is reached. Since very few experiments have been conducted on multicellular organisms to determine half-saturation coefficients directly, irrespective of whether the taxa in question is a plant or animal (Mulder and Hendriks, 2014), we calibrate K_{ij} by minimizing the deviation between length-at-age from model output relative to an empirical length-at-age curve that accounts for different growth stanzas separated out by life stage (preflexion, flexion, postflexion, and pelagic juveniles; Laidig et al., 1991). Tuning was achieved in a stepwise fashion by first calibrating the half saturation coefficient for life stage i before moving to life stage i+1 so that life stage transitions were achieved at the same age and size reported by Laidig et al (1991). Further, we assumed that life stage transitions were deterministically driven by length thresholds, rather than stage-based transition probabilities typical of structured matrix population models (Caswell, 2001) or through morphological developmental changes (Downie et al., 2020). We leveraged an empirical length-to-weight curve over the same life stages (Norton et al., 2001) to convert the state variable of the bioenergetics model (weight in grams) to standard length (SL) of fish (mm). In this way, while the parameterization of the consumption parameters, and the rest of the bioenergetics parameters for that matter, are meant to loosely represent a general rockfish, the calibrated consumption equation most closely matches that of shortbelly rockfish during four early life history stages, and as such likely provides appropriate estimates for many of the other co-occuring winter spawning rockfish, for which pelagic juvenile stages typically have comparable growth rates (Woodbury et al. 1991, Field, unpublished data).

2.2.2. Respiration

Respiration (R), or the rate of oxygen consumption during metabolic processes, is formulated in relation to body weight, seawater temperature, and activity due to swimming. The allometric function is given by:

$$R = a_R \cdot W^{b_R} \cdot F_R(T) \cdot ACT \cdot 5.258 \tag{16}$$

where a_R and b_R are the intercept and slope of the allometric relationship between resting respiration (g O_2 · g fish^{-1} · d^{-1}) and W (g fish), $F_R(T)$ is the temperature dependence function for respiration, T is the temperature of seawater, ACT (dimensionless) is the metabolic cost due to swimming (applied as a scalar factor to respiration), and 5.258 is the standard conversion factor used in bioenergetics models to convert from g O_2 · g fish^{-1} · d^{-1} to g fish · g fish^{-1} · d^{-1} (Kitchell et al., 1977; Hewett and Johnson, 1987; 1992; Hanson et al., 1997; Deslauriers et al., 2017). We employ a hump shaped function to relate temperature to respiration:

$$F_R(T) = V^X \cdot e^{X \cdot (1 - V)}, \tag{17}$$

where:

$$V = \frac{RTM - T}{RTM - RTO}, \tag{18}$$

$$X = \frac{Z^2 \cdot \left(1 + \left(1 + \left(\frac{40}{Y}\right)^{0.5}\right)^2\right)}{400}, \tag{19}$$

$$Z = \ln RQ \cdot (RTM - RTO), \tag{20}$$

$$Z = \ln RQ \cdot (RTM - RTO). \tag{21}$$

Here T is the seawater temperature. RTO and RTM are the optimal and maximum temperature for routine metabolism, respectively. RQ approximates the standard Q10 (i.e., rates double for each 10C temperature increase). Since fish in the preflexion stage do not have much swimming capability (Kashef et al., 2014), we assume that their activity is minimal and assign ACT a value of 1. However, for flexion, postflexion, and pelagic juvenile stages, we assign values of 1.8, 1.7, and 1.6,

which are similar to those used by Rose et al., (2015) for northern anchovy (Engraulis mordax), and assumes that the energetic costs to mobility decrease with ontogeny (Leis, 2007).

2.2.3. Specific Dynamic Action

Specific dynamic action (SDA) is the energy cost associated with the digestion of food. The percentage of total energy consumed that is used to digest food is believed to be relatively conserved, but the exact amount of energy lost to digestion is contingent on the amount of food consumed after accounting for egestion:

$$SDA = sda \cdot (C_{rel} - EG). \tag{22}$$

where sda is the specific dynamic action coefficient (dimensionless), C_{rel} is the realized consumption (g prey · g fish^{-1} · d^{-1}) and EG is egestion (g prey · g fish^{-1} · d^{-1}).

2.2.4. Egestion and Excretion

Egestion (fecal waste; EG) is the constant proportion (a_F) of food consumed that is indigestible and is formulated as such:

$$EG = a_F \cdot C_{rel}. \tag{23}$$

Excretion (nitrogenous waste; EX) is formulated as a constant proportion (a_E) of consumption minus egestion (i.e. assimilation):

$$EX = a_E \cdot (C_{rel} - EG) \tag{24}$$

2.3. Empirical Data

Most California rockfish are winter or early spring spawners (Wyllie-Echeverria 1987, Love et al. 2002), and while the period of parturition is generally thought to be fairly constant by species, there is considerable variability in the timing of successful recruitment, as illustrated by variability in the birthdate distributions of surviving pelagic juveniles (Woodbury and Ralston, 1991; Lenarz et al., 1995). To initialize the bioenergetics model at the median date of parturition of surviving juveniles, we analyzed daily growth rings of sagittal otoliths (earbones) to determine birthdate frequency distributions from shortbelly specimens who survived early larval stages and were caught in the Rockfish Recruitment and Ecosystem Assessment Survey (RREAS) midwater trawls as pelagic juveniles. The decision to initialize the bioenergetics model at the observed median date of parturition of survivors, rather than during the peak period of parturition (February; Wyllie-Echeverria 1987, Love et al. 2002), is so that we can align the environmental conditions in the model that would promote survival of shortbelly and hence so we can compare growth trajectories with the observed length-at-age curve of Laidig *et al.* (1991). RREAS has conducted annual midwater trawls in central California (36.5°N-38.2°N) from 1983-present and samples the micronekton assemblage from May-mid June (Sakuma et al., 2016; Field et al. 2021).

Daily ages are obtained from a subset of the collected fish through otolith microstructure analyses. Early years (1988-1992) are analyzed by Woodbury and Ralston (1991) and Lenarz et al. (1995) and we update birthdates to 2010 here. Briefly, sagittal otoliths are extracted, cleaned, and mounted on microscope slides using CrystalBond adhesive. Aluminum oxide films are utilized to hand polish otoliths down to a flat plane for better visualization. A compound microscope (25 – 100x magnification) and Image-Pro Premier imaging software (Media Cybernetics) are used to visualize otolith microstructure. As otolith formation and growth band-pair deposition begins during embryogenesis, the dark growth band denoting birthdate, the extrusion check (a distinctly darker band that forms the day the larvae are extruded from the mother), is identified to begin age determination. The concentric dark growth bands post-extrusion check through to the terminal edge of the otolith are counted to determine fish age using standard procedures (Stevenson and Campana, 1992).

Subtracting the age of a fish from the date of capture gives an individual's birthdate. To back-calculate birthdates for all individuals (aged and unaged), we developed a length-at-age relationship using SL for all individual specimens that were aged. To account for interannual differences in growth, we fit linear regression models to each year with sufficient data. We used the overall length-at-age relationship (all years) for years that did not have age data but had length frequency data (1999, 2000 and 2002). The overall median birthdate of pelagic juveniles that survived from parturition to being caught in the survey, after accounting for interannual changes in growth, were used to initialize the start date of model simulations.

We compared spatial patterns of juvenile growth potential from the 2D Eulerian version of the coupled ROMS-NEMUCSC and bioenergetics model (see 2.4 Simulations) with spatial patterns of juvenile shortbelly abundance from the RREAS. To estimate observed spatial effects, we fit a delta-generalized linear model (Δ-GLM) to raw catch data over 1988-2010 (Stefánson, 1996; Dick, 2004; Maunder and Punt, 2004). A Δ-GLM first fits a binomial presence/absence model and then the probability of a presence is multiplied by the estimated mean conditioned on a positive observation from a lognormal model with zero catches removed. We included year, station, and period (based on binned intervals of Julian day, to account for seasonality) as main effects following Ralston et al. (2013) and Schroeder et al. (2019). Station effects were then mapped to characterize empirical spatial distribution and to compare with a 2D Eulerian spatial growth potential simulation.

2.4. Simulations

A 0-D version of the bioenergetics model was used to calibrate half-saturation coefficients in Equation 14 across four early life stages (preflexion, flexion and postflexion larvae, and pelagic juveniles). To calibrate the model, we minimized the deviation between length-at-age produced by the model with that of an empirical length-at-age relationship accounting for life stage-specific growth stanzas (Laidig et al., 1991) by calibrating life stage i before moving to life stage i+1 so that the lengths separating each life stage in the model deterministically matched the same length and age of observations. The 0-D simulation was initialized on the median birthdate derived from otolith microstructure analysis over the period 1988-2010 and ran for 150 days, which is roughly the age at which pelagic juveniles settle out from the water column and recruit to their adult habitat (Love et al., 2002). Wet weight was updated each day using daily climatological temperature and prey concentration (1988-2010) at 30 m depth over 36°N-39°N, 124°W-121.5°W. Since fish cannot shrink in length, but can lose weight, we held length constant if a fish lost weight. Length would resume increasing once their weight returned to their expected weight-at-age. Therefore, fish could get skinny and be in poor condition or be fat and in good condition. We saved the following variables to output files: realized consumption (ZS, ZL, ZP, and total), proportional consumption (ZS, ZL, ZP, and total), egestion, excretion, specific dynamic action, respiration, mass-specific growth, growth, weight-at-age, and length-at-age.

A 2-D version of the model was implemented over the RREAS sampling area (36°N-39°N, 124°W-121°W) to examine spatial patterns of growth potential in response to the spatial climatology (1988-2010) of temperature and prey availability. Bioenergetics formulations were embedded into the center of each grid cell at 30m depth and growth trajectories tracked for 150 days in a Eulerian sense. Thus, we model the growth potential throughout the central California region to assess what growing conditions would have been had a fish occupied a particular grid cell (Brandt et al., 1992; Henderson et al., 2019). Composite growth maps were produced for qualitative comparisons with empirical data by taking the mean of daily growth (in weight) across each of the four life stages for each grid cell in the model domain.

2.5. Sensitivity Analysis and Scenario Tests

2.5.1. Individual Parameter Perturbation

We conducted a sensitivity analysis using individual parameter perturbation (IPP) on the 0-D climatology simulation to quantify uncertainty in the standard parameters of the bioenergetics model (Bartell et al., 1986). Each parameter was allowed to vary by +/- 5%, +/- 10% and +/- 20% of the control run values, which are standard sensitivity perturbations explored in other sensitivity analyses of bioenergetics models (Hartman and Kitchell, 2008). Length-at-age plots between the control run and each perturbation were plotted to visually compare growth trajectories. Model bias was calculated over each 150-day simulation by subtracting the length-at-age of the IPP simulation from the control run and standardized by dividing by length-at-age of the control. Overall model bias for each perturbation experiment was calculated by summing up the square root of daily model bias (analogous to sum of squares). We refer to the overall model bias as the total sum of squares (TSS). To examine the directionality of model bias, we calculate the ratio of change (ROC) as the difference in standard length for the final day of the simulation for an IPP run minus the control, standardized by the standard length of the control run at the final day of the simulation.

2.5.2. Scenario Tests

We performed a scenario test on the bioenergetics forcing factors to explore how changes in temperature and prey concentration affect model predictions and to make inference about future climate conditions. First, we examined the effect of holding temperature (prey) constant at the mean value (i.e., took the mean of prey (temperature) over the 150-day time series used in the 0-D control run) and allowed prey (temperature) to vary daily (same forcing as control run) to understand the influence of daily and seasonal variability in forcing variables on growth performance, relative to fixed temperature or prey concentration. Next, four separate scenario tests were conducted on different combinations of constant temperature and prey availability to understand the influence of novel conditions on growth performance. Scenario 1 allowed temperature to vary about the mean (+/- 5%, +/- 10% and +/- 20%) while holding prey concentrations constant at the mean. Scenario 2 allowed prey concentrations to vary about their respective mean (same as Scenario 1) while holding temperature constant at the mean. Scenario 3 allowed temperature and prey concentrations to vary (magnitude of change same as Scenario 1 & 2), but in equal fashion; temperature and prey concentrations were both added to, or subtracted from, the mean simultaneously. Finally, Scenario 4 allowed temperature and prey concentrations to vary but in opposite directions (i.e., add 5% of temperature and subtract 5% of prey concentrations and vice versa). We report ROC for all combinations of each scenario test.

3. Results

3.1. Simulated historical temperature and prey concentrations

Temperature, microzooplankton (ZS), mesozooplankton (ZL) and predatory zooplankton (ZP) from the 23-year climatology of ROMS-NEMUCSC for the focal area of our study exhibits marked seasonal cycles (Fig. 2-3). When spatially averaged over the study region to produce the 0-D climatology at 30m depth, temperature decreases from January 1st-May14th, increases until the end of September, before decreasing for the remainder of the year (Fig. 2). The thermocline is shallowest from April to July during peak upwelling and stratification is strongest from July to mid-November (Fig. 3). As expected, temperature decreases with latitude, with the coolest temperatures (~10-11°C) at the northernmost latitudinal range (38-39°N) from late March to July (Fig. 3), and the warmest temperatures (~14-15.5°C) being found at the southernmost latitudes (36-37°N) during the Fall (Fig. 4). The coolest temperatures occur closest to the coast during the winter and spring months and increase with distance offshore (not shown). These temperature patterns reflect the seasonality of coastal wind-driven upwelling and in turn drive primary and secondary productivity.

Zooplankton concentrations produced by NEMUCSC exhibit seasonal patterns (Fig. 2-3). All three zooplankton functional groups increase from a minimum beginning on January 1st but peak at different times

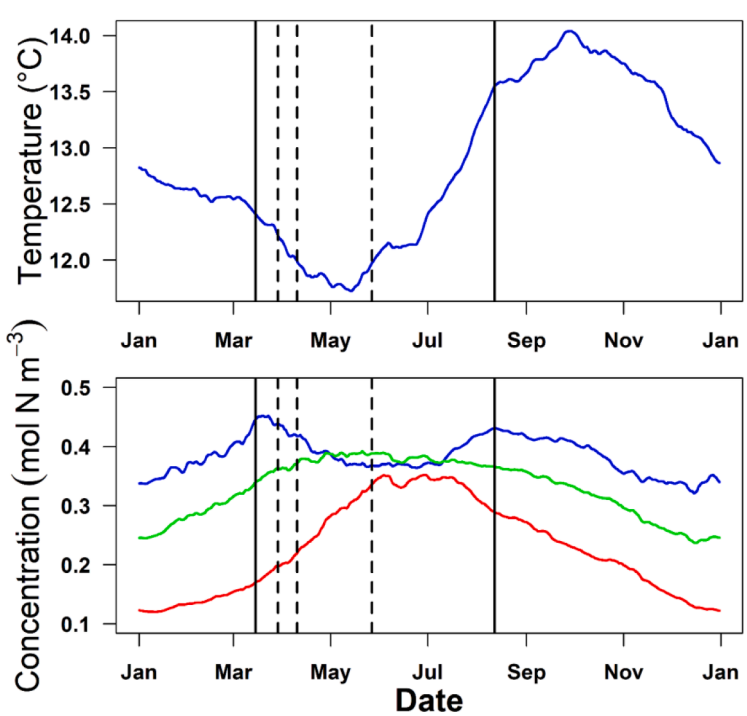

Fig. 2. 30m depth 0-D climatological (1988-2010) time series of temperature and concentration (mol N m^{-3}) of microzooplankton (ZS; blue), mesozooplankton (ZL; green), and predatory zooplankton (ZP; red) used to force the bioenergetics model. Solid vertical lines denote the beginning and end dates of the bioenergetics simulation. Dashed vertical lines denote the transition from preflexion-to-flexion, flexion-to-postflexion, and postflexion-to-juvenile stages.

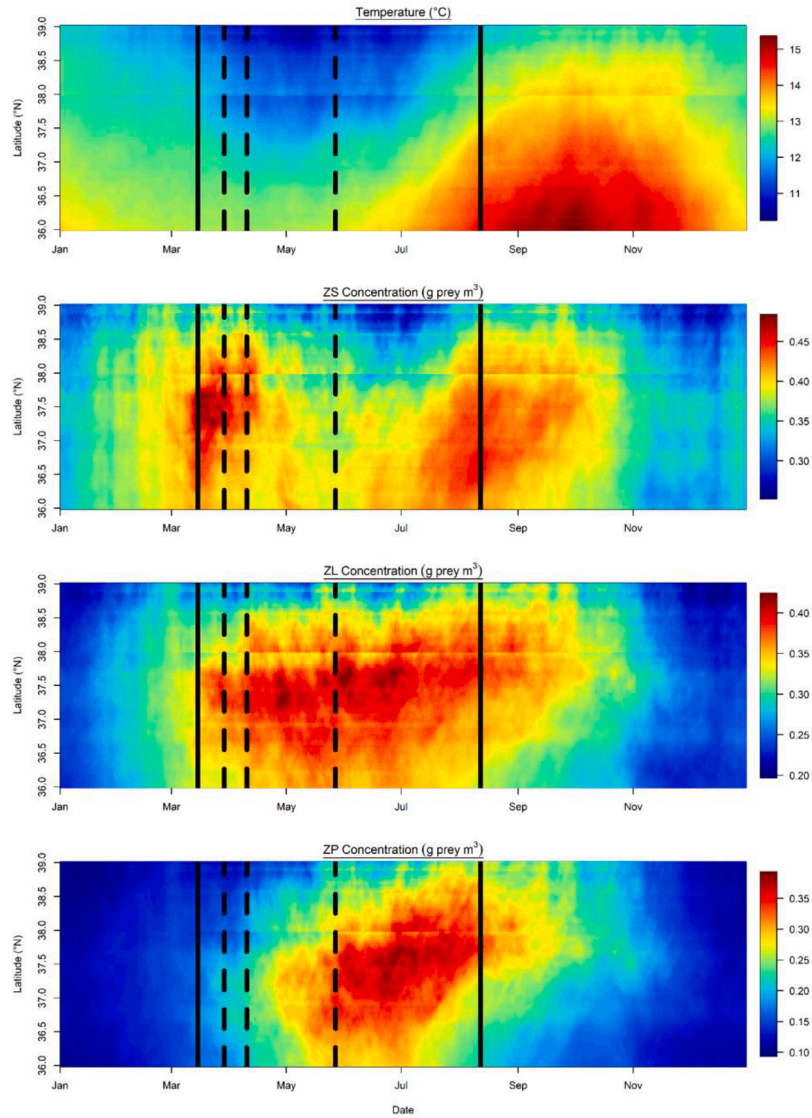

Fig. 3. Latitudinal Hovmöller plots of climatological temperature, microzooplankton (ZS), mesozooplankton (ZL), and predatory zooplankton (ZP) from ROMS-NEMUCSC. Solid vertical lines denote the beginning and end dates of the bioenergetics simulation. Dashed vertical lines denote the transition from preflexion-to-flexion, flexion-to-postflexion, and postflexion-to-juvenile stages.

(Fig. 2); ZS concentration is greatest in mid-March (0.45 mol N m^{-3}); ZL is greatest in mid-May (0.39 mol N m^{-3}); and ZP is greatest in late-June (0.35 mol N m^{-3}). Horizontally, peak zooplankton concentrations occur at ~37.5 °N and between 123-122.25 °W (Fig. 3), which is located just south of the Gulf of Farallones, near Pioneer Canyon (Fig. 1).

3.2. Birthdate Distribution and 0-Dimensional Bioenergetics Climatology

Otolith microstructure analysis of pelagic juvenile shortbelly rockfish caught in the RREAS midwater trawls over the period 1988-2010 estimated a median back-calculated birthdate of March 15th, with a standard deviation of 24 julian days (n = 8,645; Figure S2). The frequency of back-calculated birthdates had a bimodal distribution with a peak occurring in mid-February and a second peak in late-March/early-April. The median birthdate was used as the day of year to initialize the 0-D climatology bioenergetics model.

Ontogenetic changes in respiration, consumption and subsequent growth are partially driven by daily and seasonal changes in temperature and prey availability (Figs. 2, 3 and 4A-B). Temperature declined from the start to three quarters of the way through the postflexion larval stage, after which temperature increased and continued to increase throughout the pelagic juvenile stage (Figs. 2, 3 & 4A). 100% of the preflexion larval diet comes from ZS (υ_{11}), with ZS comprising 50%, 50%, and 20% of flexion (υ_{12}), postflexion (υ_{13}) and pelagic juvenile (υ_{14}) diets, respectively (Table 1). ZS concentration was relatively high and stable throughout the simulation. The preflexion stage coincided with the highest ZS concentration (~0.45 mol N m^{-3}), flexion occurred when ZS concentration were slightly decreased (~0.43 mol N m^{-3}), while postflexion and pelagic juvenile stages took place when ZS were slightly further decreased (~ 0.38 mol N m^{-3}; Fig. 2, 3 & 4B). ZL comprises 0%, 50%, 50% and 30% of preflexion (υ_{21}), flexion (υ_{22}), postflexion (υ_{23}) and pelagic juvenile (υ_{24}) diets, respectively (Table 1). The flexion stage coincided when ZL concentrations were relatively high and stable (~0.36 mol N m^{-3}), with the postflexion stage occurring when ZL were slightly increased (~0.38 mol N m^{-3}) and the pelagic juvenile stage was slightly decreased from the preceding life stage (~0.37 mol N m^{-3} (Fig. 2, 3 & 4B). ZP comprises 0% of the diet of preflexion (υ_{31}), flexion (υ_{32}), and postflexion (υ_{33}) larval stages and 50% of pelagic juvenile (υ_{34}) diet (Table 1). During the pelagic juvenile stage ZP concentration was at a maxima but declined slightly during the last 20 days of the simulation (Figs. 2, 3 & 4B).

The final calibration of the ELS bioenergetics model yielded a length-

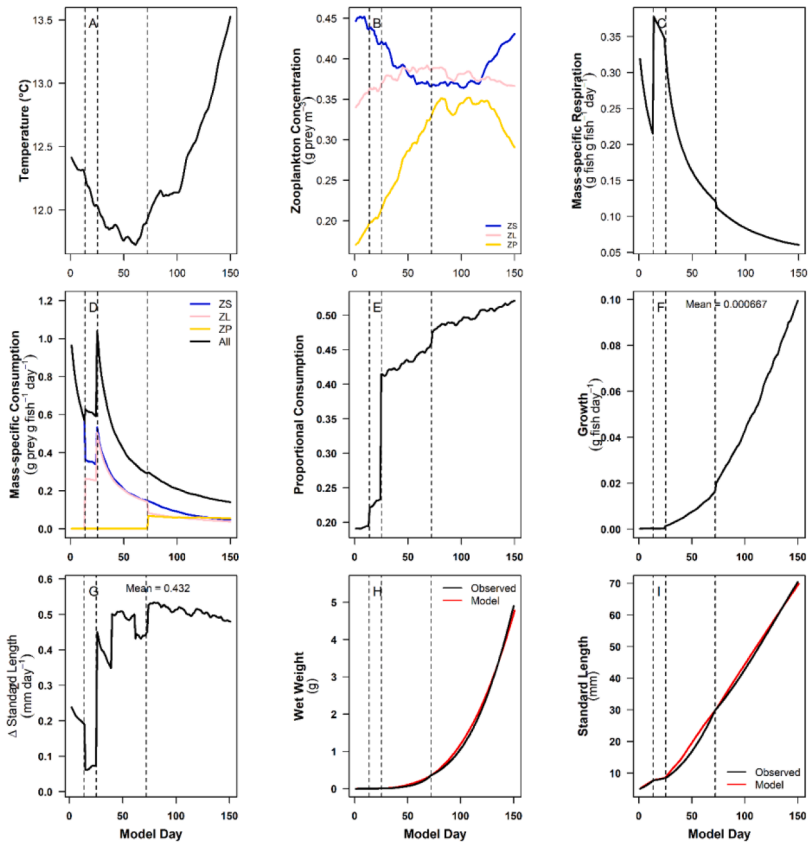

Fig. 4. Bioenergetics processes of the 150-day 0-D climatology simulation. (A) Daily temperature at 30m depth used to force the bioenergetics model. (B) Daily concentrations (g prey m^{-3}) of small zooplankton (ZS; blue line), large zooplankton (ZL; pink line), and predatory zooplankton (ZP; gold line) used to force consumption in the bioenergetics model. (C) Total daily mass-specific respiration (g fish $fish^{-1}$ day^{-1}) resulting from the bioenergetics simulation. (D) Daily mass-specific consumption (g prey g $fish^{-1}$ day^{-1}) given temperature and prey concentrations. (E) Proportion of maximum allometric consumption (dimensionless). (F) Daily growth in weight (g fish day^{-1}) and (G) daily growth in length (mm day^{-1}). (H) Weight-at-age (g) and (I) length-at-age from the bioenergetics simulation (red lines) relative to empirical size-at-age (black lines; Norton et al., 2001; Laidig et al., 1991).

at-age curve that closely matched the observed length-at-age curve for shortbelly rockfish (Fig. 4I). Importantly, the starting and ending standard lengths for each life stage (preflexion larvae, Stage I; flexion larvae, Stage II; postflexion larvae, Stage III; and pelagic juvenile, Stage IV) from the simulation closely match that of the empirical length-at-age curve, implying that the model, on average, reproduces ontogenetic developmental stages at the same age (Stage I <14 days old; Stage II < 26 days old; Stage III < 73 days old; Stage IV > 74 days old). The model produces a mean growth rate of ~0.667 mg day^{-1} (0.432 mm SL day^{-1}; Fig. 4F-G) and closely tracks the empirical growth trajectory across all ontogenetic stages (Fig. 4H-I). Within ontogenetic stages, average modeled growth for preflexion larvae is ~0.21 mm SL day^{-1} (~0.25 mg day^{-1}), ~0.10 mm SL day^{-1} (~0.37 mg day^{-1}) for flexion larvae, 0.45 mm SL day^{-1} (~8.12 mg day^{-1}) for postflexion larvae, and ~0.51 mm SL day^{-1} (~57 mg day^{-1}) for pelagic juveniles. In comparison, the empirical growth measurements for preflexion larvae are ~ 0.21 mm SL day^{-1}, ~0.08 mm SL day^{-1} for flexion larvae; ~0.47 mm SL day^{-1} for postflexion larvae, and 0.52 mm SL day^{-1} for the pelagic juvenile stage. However, along a growth trajectory, the model slightly overestimates growth for postflexion larvae as the model produces a more linear change in SL while the empirical trajectory is convex.

Ontogenetic changes occur for total mass-specific respiration rate (g fish · g $fish^{-1}$ · d^{-1}), with the largest relative rate of oxygen consumption (~35%) happening during the flexion stage and declining thereafter (Fig. 4C). These stepped changes in total mass-specific respiration are due to ontogenetic changes in activity levels (ACT; Table 1). Mass-specific consumption rates (g prey · g $fish^{-1}$ · d^{-1}) are greatest at the transition between flexion and post-flexion stages (Fig. 4D). Ontogenetic changes in mass-specific consumption are primarily due to changes in half-saturation coefficients (K_{ij}; Table 1) but are also attributed to changes in dietary preferences (v_{ij}, Table 1) and to seasonal changes in temperature and prey concentrations (Fig. 1). Proportional consumption relative to maximum consumption is at a minimum for newborn larvae (~20%; preflexion larvae) and increase throughout ontogeny (up to ~50% by the end of the pelagic juvenile stage), with a pronounced, and stepped, increase at the transition from flexion to postflexion larval stages (Fig. 4E).

3.3. Sensitivity Analysis: Individual Parameter Perturbation

Sensitivity of bioenergetics parameters by individual parameter perturbation (IPP) are quantified as the ratio of change (ROC (Fig. 5). IPP identifies the allometric slope and intercept of maximum consumption (cb and ca, respectively) as having the largest effect on growth. The relative influence of decreasing the values of cb and ca are larger compared to an increase because growth is slowed under smaller values, and thus, more time is spent in earlier larval stages where mass-specific growth rates are slower. A similar pattern is found for the slope and intercept of allometric respiration (rb and ra, respectively), and the optimal temperature for respiration (RTO), which had the third, fourth and fifth largest effect, respectively (Fig. 5). The temperature-dependence on maximum consumption parameter describing the peak of the ascending limb of the temperature-dependence function (te2), maximum temperature for respiration (RTM) has the smallest effect on growth (Fig. 5). All other parameters tested in the sensitivity analysis have a modest effect on the final size of fish (Fig. 5).

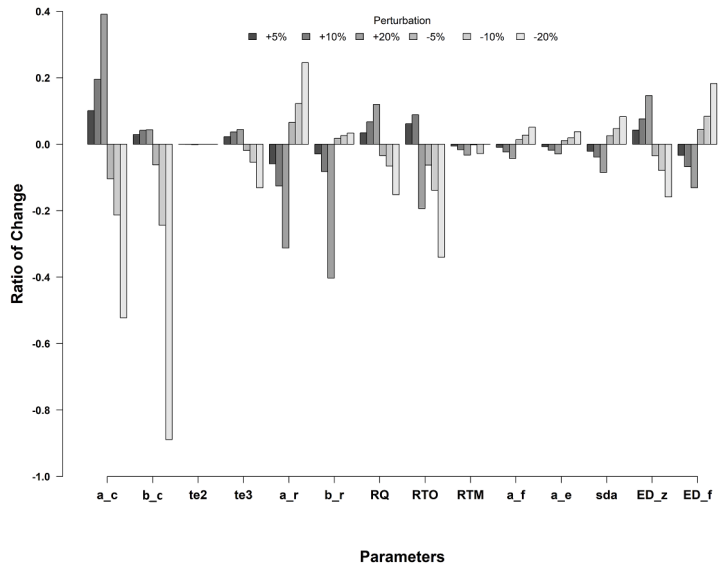

Fig. 5. Ratio of Change (ROC), or the ending standard length (SLend) of the perturbed simulation minus SLend control, divided by SLend control, for the individual parameter perturbation (IPP). Refer to Table 1 for a description of each parameter and their nominal value.

3.4. Scenario Tests: Sensitivity of Forcing Factors

When holding temperature constant and allowing prey concentrations of ZS, ZL and ZP to vary daily (i.e. same as in control runs), the final SL did not vary much from the control (ROC = 0.002), nor did the trajectory over the 150 day simulation period (TSS = 0.48). When holding prey constant and allowing temperature to vary daily, the final SL was slightly smaller than the control (ROC = -0.019), however, the growth trajectory over the simulation period was faster compared to the control (TSS = 5.031). When holding both temperature and prey concentrations constant about their mean, length-at-age was consistently higher (TSS = 5.95), however, the final length-at-age was slightly smaller (ROC = -0.027).

Increasing mean temperature causes the largest discrepancies compared to a decrease in temperature or changes to prey concentration (Fig. 6). For example, in Scenario 1, increasing temperature by 20% causes fish to grow more slowly, resulting in fish that were ~40% smaller by the end of the simulation (ROC = -0.40; Fig. 6). In contrast, when decreasing temperature by 20%, fish grow faster and are ~14% larger by the end of the simulation (ROC = 0.135). By comparison, decreasing prey concentration by 20% (Scenario 2) causes fish to grow more slowly with the final length of fish being 27% smaller than the control (Fig. 6). Increasing prey concentration has marginal improvements to growth with a 20% increase in prey concentration resulting in fish that are 16% larger at the end of the simulation (Fig. 6). These results suggest that temperature has a larger impact on growth performance compared to prey availability and the directionality of change matters more than the magnitude of change; increasing (decreasing) temperature (prey concentration) has a disproportionate negative influence on growth compared to decreasing temperature or increasing prey concentration. This result is strengthened by the ROC scores for Scenario 3 and Scenario 4. Scenario 3, which allows both temperature and prey concentrations to vary in the same direction, leads to a dampening effect; increasing temperature and prey concentration by

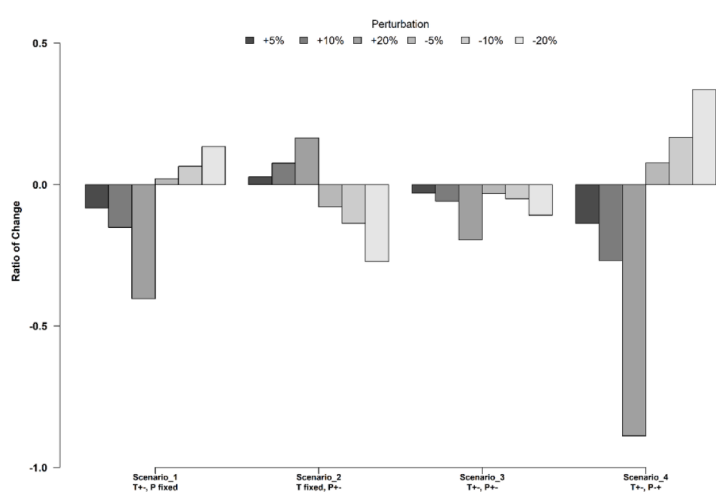

Fig. 6. Ratio of Change (ROC) of the input scenario tests. In Scenario 1, temperature to vary about the mean (+/- 5%, +/- 10% and +/- 20%) while holding prey concentrations constant at the mean. In Scenario 2, prey concentrations to vary about the mean while holding temperature constant at the mean. In Scenario 3, temperature and prey concentrations to vary, but in equal fashion; temperature and prey concentrations were both added to, or subtracted from, the mean simultaneously. In Scenario 4, temperature and prey concentrations to vary but in opposite directions (i.e. add 5% of temperature and subtract 5% of prey concentrations and vice versa). Importantly, the three bars on the left of Scenario_4 are the ROC scores when temperature additions were made and prey concentration reduced, and vice versa for the three bars on the right.

20% leads to a 20% decrease in the final length of fish at the end of the simulation, while decreasing both temperature and prey concentration leads to a ~10% decrease in final length (Fig. 6). However, in Scenario 4, when temperature increases by 20% and prey concentration decreases by 20%, fish are 89% smaller at the end of the simulation relative to the control (Fig. 6). Decreasing temperature by 20% and increasing prey concentration by 20% leads to a ~34% increase in final length (Fig. 6). Importantly, when a scenario led to a decrease in growth, deviations were amplified because length-based stage transitions caused fish to get 'stuck' in the slow growing flexion stage and were unable to transition to the faster growing postflexion stage. The ROC for this situation was always -0.89.

3.5. 2-D Eulerian Climatology and Pelagic Juvenile Spatial Distribution

The Eulerian climatology (1988-2010) of spatial patterns of growth potential for preflexion, flexion, and postflexion larvae, and pelagic juveniles reveals heterogeneity of growth potential with different spatial patterns associated with each life stage (Fig. 7). The spatial pattern of growth potential is patchiest for preflexion larvae with maximum growth (~0.4-0.45 mg day^{-1} (0.3-0.4 mm day^{-1})) constrained to a localized region of the mid and outer shelf to the south of the Gulf of Farallones Islands, containing Pioneer Canyon and Ascension Canyon (Fig. 7A). A similar pattern occurs for flexion larvae, albeit over a slightly larger area, with maximum growth rates of ~0.6 mg day^{-1} (0.2-0.25 mm day^{-1} (Fig. 7B). Spatial patterns of growth potential for postflexion larvae are most homogeneous with maximum growth of 9-10 mg day^{-1} (0.5-0.6 mm day^{-1}) over the shelf break along the entire latitudinal extent of the study region (Fig. 7C). Pelagic juvenile growth potential is slightly more constrained to the shelf break compared to postflexion larvae, with maximum growth rates of 70 mg day^{-1} (0.5 mm day^{-1}) just offshore of the greater Farallones region and monotonically declining to 25 mg day^{-1} (~0.3 mm day^{-1}) towards the southwest extent of the model domain (Fig. 7D). Collectively, while there is considerable variability in growth performance across individual grid cells (Fig. 7), an average of all growth trajectories fits well within empirical growth estimates, noting a slight overestimation of mean growth potential for postflexion larvae (Fig. 8), further supporting the notion that the model is well calibrated to handle a range of temperature and prey conditions. Station-effects from the Δ-GLM of pelagic juveniles caught by midwater trawls in the RREAS reveals peak abundance of shortbelly over the 200m isobath, just to the south of the Gulf of Farallones, at two stations near Ascension Canyon, and in the outer Monterey Bay area (Fig. 9), which is consistent with the spatial patterns of

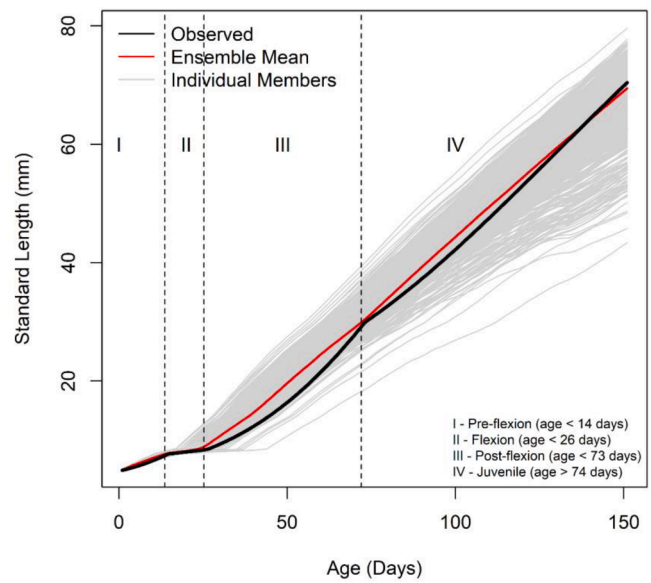

Fig. 8. Standard length (SL) at age ensemble for all 3,750 individuals tracked in the 2D Eulerian climatology (grey lines). The mean of all individuals (red line) is plotted relative to the empirical length-at-age curve (black line) from Laidig et al., (1991). Vertical dashed lines denote transitions between life stages.

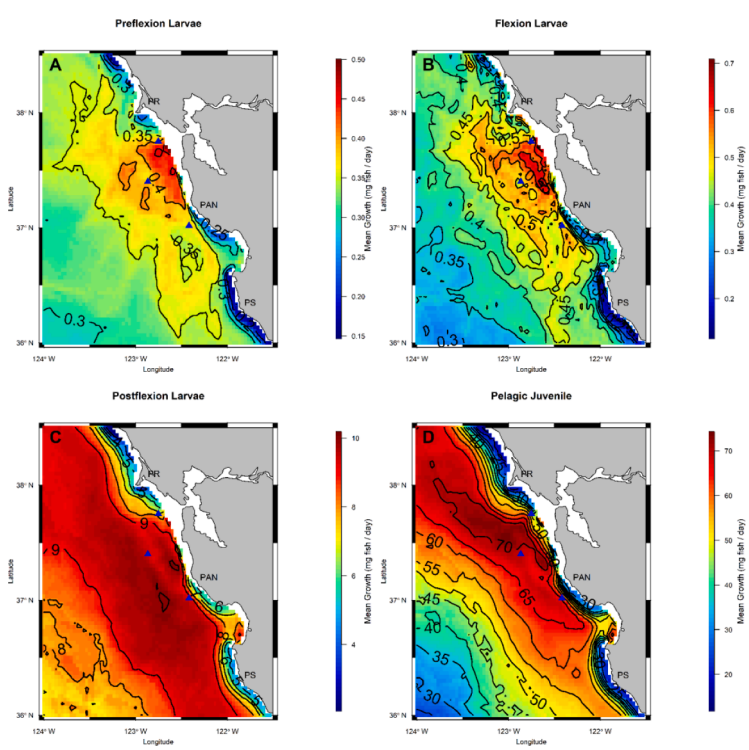

Fig. 7. Mean stage-specific growth potential maps of the 2-D Eulerian climatology for (A) preflexion, (B) flexion, (C) and postflexion larvae, and (D) the pelagic juvenile stage..

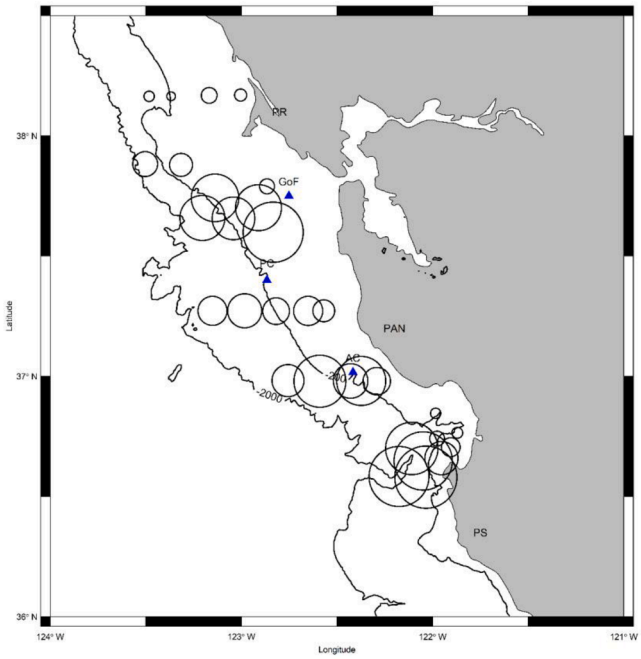

Fig. 9. Pelagic juvenile shortbelly rockfish (*Sebastes jordani*) station-effects from Δ-GLM of the core stations from the Rockfish Recruitment and Ecosystem Assessment Survey over the period 1988-2010. The size of the circle indicates the relative abundance at that station. Major promontories are labeled on land (PR = Point Reyes; PAN = Point Año Nuevo; PS = Point Sur) and the Gulf of Farallones (GoF) and two canyon systems (blue diamond: PC = Pioneer Canyon; AC = Ascension Canyon) important to shortbelly life history.

growth potential for the pelagic juvenile stage (Fig. 7D).

4. Discussion

This study presents a highly resolved ontogenetic bioenergetics model for the ELS of an ecologically important fish in the central California Current System (CCS), the shortbelly rockfish. When accounting for ontogenetic dietary preferences and feeding rates through a realized consumption term (Rose et al., 1999a; 1999b), the baseline bioenergetics model presented here sufficiently reproduces empirical growth stanzas of preflexion, flexion, and postflexion larvae and pelagic juvenile shortbelly rockfish in the central CCS (Laidig et al., 1991) which would not have been recovered if stage-specific adaptations to the model were ignored. Growth during ELS's can contribute to differential survival from year-to-year and lead to orders of magnitude changes in recruitment (Houde, 2008). At what ELS stage a bottleneck to survivorship occurs from growth-dependent mortality can vary in both space and time depending on the timing of reproduction, successional changes in preferred prey types, and changes in environmental forcing that affects growth rates (Peck and Hufnagl, 2012). A model that accounts for highly resolved changes in ELS growth stanzas, such as the one presented here, can help to elucidate at what early life stage growth-dependent mortality is most pronounced under a given set of environmental conditions. Conversely, failure to account for ontogenetic variability within mechanistic growth models can obscure growth-dependent survival if the directionality of the relationship changes across life stages (e.g., slow growth, high survival during early larval stages v. fast growth, high survival during later ELS's; Robert et al., 2023).

Some interesting patterns emerge when comparing the seasonality of forcing factors with the timing of model initialization and developmental transitions. First, the optimal temperature for consumption (~12°C) occurs at the beginning of March, just prior to model initialization. While upwelling is somewhat persistent in central California (36-39°N), the spring transition dates for this region occur on average during February (Bograd et al., 2009), which preconditions the ecosystem with cool waters and plankton production that is advantageous to shortbelly rockfish prior to the median parturition date of March 15th (Schroeder et al., 2009; 2013; Black et al., 2010). First feeding preflexion larvae are obligate feeders on small zooplankton which peak in abundance near the start of the simulation. Similarly, as shortbelly progress through ontogeny, the proportion of large zooplankton and krill (ZP) becomes increasingly important to diet and the temporal aspect of this prey switching mirrors the phenology/-succession in prey concentration predicted by the ROMS-NEMUCSC historical simulation. Taken together, this suggests, at least in a climatological sense, a temporal match between prey production, the timing of average reproduction leading to survival of pelagic juveniles (based off otolith microstructure analysis), and transitions between developmental stages. The match-mismatch hypothesis posits year class success is enhanced when there is a temporal overlap between fish larvae and zooplankton prey (Cushing 1969; 1982; 1990; Durant et al., 2005; 2007; 2013). However, the CCS is highly dynamic (Checkley and Barth, 2009) over multiple scales (Chavez and Messié, 2009) and exhibits pronounced interannual variability in plankton production (McGowan et al., 1998). If fish spawning times are fixed, or spatially invariable, a mismatch between predator and prey can occur, causing recruitment failure. For example, atmospheric blocking of poleward winds in 2005 (Sydeman et al., 2006) delayed coastal upwelling in the central CCS (Schwing et al., 2006) which led to reduced plankton production in late winter and early spring (Thomas and Brickley, 2006; Jahncke et al., 2008) when peak rockfish production occurs (Love et al., 2002). These series of events coincided with low biomass anomalies of pelagic juvenile shortbelly rockfish for our study region (Ralston and Stewart, 2013), possibly owing to a temporal mismatch between peak reproduction and prey availability. Over longer time scales, however, natural selection should favor the timing of life history events that align with the long-term seasonality of environmental conditions (Ji et al., 2010; Giménez, 2011; Durant et al., 2019). Using a temperature and zooplankton climatology from a coupled physical-biogeochemical simulation to force a bioenergetics model that accounts for ontogenetic changes in feeding parameters fortuitously demonstrates the temporal alignment between temperature, zooplankton succession, and the timing of developmental transitions, inline with the match-mismatch hypothesis.

Empirical growth rates for ELS rockfish in the CCS are known to vary interannually (Crane, 2014; Fennie et al., 2023; Johnson et al., 2001; Lenarz et al., 1995; Wheeler et al., 2017). For shortbelly rockfish specifically, empirical growth rates of surviving pelagic juveniles during the 1980s ranged between 0.524 mm/day to 0.638 mm/day (Woodbury and Ralston, 1991), which are within our predictions for the same life stage. However, ontogenetic changes in growth are known to occur for marine fishes (e.g. Hare and Cowen, 1995) and we found that somatic growth of larvae is slower, especially for flexion larvae, than that of pelagic juveniles. Considerable developmental and physiological changes occur during larval metamorphosis, e.g. during flexion, the posterior end of the notochord turns upward and fins begin to differentiate, changing the rate of somatic growth (Blaxter, 1969; Ricker, 1979). The physiological response for flexion larvae, in the context of our model, is an abrupt increase in mass-specific respiration (driven by an increase ACT) which must be compensated for by an increase in consumption to meet energetic demands. This has implications for the effect of temperature changes due to natural climate variability and anthropogenic climate change, and associated changes in lower trophic level productivity on growth since respiration and consumption are temperature-dependent. Moreover, we note that our parameterization of allometric formulations (e.g. respiration and consumption) did not account for ontogenetic changes, but rather our model only considers changes in observed dietary preferences (vulnerability; v_{ij}) and feeding rate parameters that

were estimated within the model (i.e. half saturation constants; K_{ij}) to account for life stage-specific growth rates. This suggests that even with a paucity of detailed species-specific experimental data on ontogenetic changes in physiology, the bioenergetics model can still generate realistic predictions of somatic growth across larval and pelagic juvenile ELS's given a highly resolved length-at-age curve with designated length-based stage transitions.

We subjected the 0-D climatological bioenergetic model to a sensitivity analysis by individually perturbing parameters at set percentages (Bartell et al., 1986). Our results indicate that the most sensitive parameters are associated with allometric consumption and respiration, which is similar to the findings of other bioenergetics sensitivity analyses (Kitchell et al., 1977; Bartell et al., 1986; Megrey et al., 2007; Brodie et al., 2016). We adopted most of our parameter values from a generic adult rockfish bioenergetic model (Harvey, 2005; 2009) and consumption parameters from settled juveniles (Boehlert & Yoklavich, 1983), which, given ontogenetic changes in physiology and allometry (Peck and Moyano, 2016), likely caused larger deviations than would have occurred if we had access to ELS specific parameters of consumption and respiration. However, we used the best available data at the time of model development. The use of a realized consumption term that accounts for seasonal changes in prey concentration (from NEMUCSC) as well as ontogenetic differences in preferred prey from field data (Sumida and Moser, 1984; Reilly et al., 1992) may offset the bias between predicted and observed length-at-age when using energetics parameters for settled juveniles and adults. Our findings could be refined with consumption and respiration experiments on the ELS of commercially and ecologically important rockfishes (e.g. Boehlert, 1978; 1981; Boehlert and Yoklavich, 1983) to get more reliable estimates of allometric parameters to reduce model uncertainty. However, logistical constraints may complicate this call as culturing the appropriate prey items for rearing larval rockfishes in a laboratory setting is a time-intensive challenging endeavor. Furthermore, care must be taken when using controlled laboratory experiments that estimate temperature-dependence parameters of performance (i.e. respiration, consumption, and activity) because of Jensen's inequality (Jensen, 1906; Ruel and Ayres, 1999). Typically, temperature- and weight-specific parameters are calculated from controlled laboratory experiments where temperatures are held constant within treatments. Performance of an individual under average temperature is different compared to the average performance in a thermally variable environment. Nonlinear averaging techniques can alleviate these biases (Bernhardt et al., 2018), but caution is still warranted because they do not account for time-dependent interactions between body temperature and physiological plasticity (Denny, 2019).

We assessed the relative influence of temperature and prey concentrations on growth through an orthogonal manipulation of respective forcing factors. Temperature had a larger effect on growth trajectories than prey concentration, but the deviance in growth rates depended on the directionality of temperature change with warmer temperatures disproportionately decreasing growth relative to cooler temperatures increasing growth. This is because increasing temperatures had a large effect on consumptive rates as the temperature moved outside of the optimum and decreased consumption; decreasing temperature, even by 20%, allowed consumption to stay within the optimum. As expected, decreasing food availability led to a decrease in growth and vice versa. Moreover, both a synergistic and antagonistic effect was found when temperature and food availability were allowed to covary. An antagonistic effect was found when forcing changed in the same direction since the relative effect of increasing (decreasing) temperature was partially offset by an increase (a decrease) in food availability. Conversely, a synergistic effect was found when temperature and prey concentration varied in opposite directions. This scenario is what is predicted for the CCS under anthropogenic climate change, specifically an increase in temperature and a possible decrease in zooplankton concentrations (Pozo Buil et al., 2021; Fiechter et al., 2021; Koenigstein et al., 2022), which according to our model, could lead to a substantial decline in growth, and under the extreme case (20% increase in temperature, 20% decrease in prey concentration), fish were unable to grow out of the flexion stage which is probably not realistic. Nevertheless, recognizing that growth is linked to mortality (e.g., the stage duration hypothesis; Houde, 1989), this scenario would lead to severe mortality and a significant decline in recruitment unless fish can move to cooler habitat with increased food production. The coastal pelagic environment of the central CCS is a biodiversity hotspot for marine predators (Hazen et al., 2013) and many species are reliant upon shortbelly rockfish and co-occurring juvenile rockfishes as a prey source (Szoboszlai et al., 2015). For example, diets of the common murre (*Uria aalge*) switch from pelagic juvenile rockfish to northern anchovy under low rockfish regimes, which results in the incidental predation of juvenile salmon that frequently co-occur with northern anchovy in coastal waters (Wells et al., 2017). However, caution is warranted in our scenario approach because of Jensen's inequality. However, when we kept prey concentration the same as in the control run and held temperature constant at its nominal value (mean of temperature throughout the duration of the simulation), length-at-age over the duration of the simulation and the terminal length at the end of the simulation was nearly the same as the control run (TSS = 0.48; ROC = 0.002, respectively). Additional research on the impacts of Jensen's inequality to bioenergetic model predictions in relation to the scale of temporal variability of temperature is needed (e.g., Holsman and Danner, 2016).

The 2-D Eulerian climatology of spatial growth potential reveals spatial patterns strikingly similar to the known distribution of reproducing adults, the dispersal of larvae, as well as the distribution of pelagic juvenile shortbelly rockfish. Interestingly, the model produced patchy spatial patterns of growth for the earliest life stages and more homogenous patterns for later ELS's. For preflexion (<14 days old) and postflexion larvae (15-26 days old), growth is maximized along the shelf break just offshore of San Francisco, near the Farallones Islands and Pioneer Canyon, and to a lesser extent, Ascension Canyon. This region is federally protected under the United States Greater Farallones National Marine Sanctuary and overlays the main spawning grounds for shortbelly rockfish, as revealed by extensive spatial sampling of recently born larvae (age 0-2 days; Ralston et al., 2003). Furthermore, nutritional dynamics of embryos from gestating females in this region contain a higher prevalence of lipids and proteins that aid in starvation resistance relative to areas to the north (i.e. Cordell Bank), suggesting this region is favorable for both larval production, and in light of our study, larval survival (MacFarlane and Norton, 1999). Spawning site fidelity is, on average, an adaptive strategy that places larvae in habitat favorable for survival (Ellersten et al., 1989). Recognizing that faster early larval growth is tied with reduced mortality (Houde, 1989), adults who reproduce in areas of enhanced growth, on average, ensure a higher probability of early life survival and life cycle closure (Cushing, 1969; Sinclair, 1988). Furthermore, as larvae progress through ontogeny, and are vulnerable to dispersal by ocean currents, survival is contingent upon starvation resistance and predator avoidance (Peck and Hufnagle, 2012). Our spatial climatology of growth reveals favorable growing conditions for postflexion larvae throughout the study area suggesting that, on average, late-stage larvae can find sufficient food to resist starvation as long as they are not advected too far offshore where zooplankton production is reduced and temperatures are warmer (Checkley and Barth, 2009). Finally, there is spatial coherence between the distribution of pelagic juveniles and the spatial pattern of maximum growth potential. The preponderance of pelagic juvenile rockfish having the ability to resist offshore advection (Larson et al., 1994; Kashef et al., 2014) along with our results, points to the possibility of pelagic juvenile rockfish behaviorally aggregating in areas that are favorable for growth, survival, and settlement. Taken together, our model generates spatial patterns of growth potential for each of the four early life stages of shortbelly rockfish that are in line with known attributes of their life history strategies which would not be quantifiable if life stage-specific

parameterizations of feeding rates and dietary preferences were ignored.

To conclude, we demonstrate, to the first of our knowledge, that a bioenergetics model with high ontogenetic resolution of the early life stages for a marine fish can produce accurate predictions of somatic growth using imperfect physiological data (i.e. adult parameters). We relied on imprecise ontogenetic parameterizations of key physiological functions (e.g. allometric metabolism) which can be offset with accurate environmental forcing, knowledge of reproductive phenology and ontogenetic changes in dietary preferences. Bioenergetic growth models that account for within ELS growth stanzas can be nested within Lagrangian individual-based models to understand the mechanisms of recruitment variability, and at what life stage(s) bottlenecks to survival occur. Mechanistic models, such as the one we present here, can be applied under the backdrop of various climate change scenarios, or be used to inform ecosystem-based fisheries management objectives.

CRediT authorship contribution statement

Mark M. Morales: Conceptualization, Formal analysis, Funding acquisition, Investigation, Methodology, Software, Validation, Visualization, Writing – original draft, Writing – review & editing. **Jerome Fiechter:** Conceptualization, Funding acquisition, Methodology, Resources, Software, Supervision, Writing – review & editing. **John C. Field:** Investigation, Data curation, Resources, Writing – review & editing. **Neosha S Kashef:** Investigation, Resources, Writing – review & editing. **Elliott L. Hazen:** Conceptualization, Funding acquisition, Supervision, Writing – review & editing. **Mark H. Carr:** Conceptualization, Project administration, Supervision, Writing – review & editing.

Declaration of Competing Interest

The authors declare that they have no known competing financial interests or personal relationships that could have appeared to influence the work reported in this article.

Data availability

Data will be made available on request.

Acknowledgements

Financial support for M.M.M. was provided by the National Science Foundation Graduate Research Fellowship Program (DGE1339067), Dr Earl H. Myers and Ethel M. Myers Oceanographic and Marine Biology Trust Research Grant, and the Friends of Seymour Discovery Center Student Research and Education Awards. Partial support for M.M.M. was provided by a grant from the National Aeronautics and Space Administration (80NSSC17K0574). The authors kindly thank Peter T. Raimondi, Sophia Simon, and two anonymous reviewers who greatly improved earlier versions of this manuscript. We are grateful to the captains, crew, technicians, and scientists who participate in the Rockfish Recruitment and Ecosystem Assessment Survey for without them the data presented would not be available.

Supplementary materials

Supplementary material associated with this article can be found, in the online version, at doi:10.1016/j.ecolmodel.2023.110575.

References

Ainley, D.G., Sydeman, W.J., Parrish, R.H., Lenarz, W.H., 1993. Oceanic factors influencing distribution of young rockfish (Sebastes) in central California: a predator's perspective. California Cooperative Oceanic Fisheries Investigations Reports 34, 133–139.

Anderson, J.T., 1988. A review of size dependent survival during pre-recruit stages of fishes in relation to recruitment. Journal of Northwest Atlantic Fishery Science 8, 55–66.

Bailey, K.M., Houde, E.D., 1989. Predation on eggs and larvae of marine fishes and the recruitment problem. In: Advances in Marine Biology. Blaxter, J., Douglas, B. (Eds.), Academic Press, Cambridge, MA, Volume 25, pp. 1-83, https://doi.org/10.1016/S0065-2881(08)60187-X.

Bartell, S.M., Breck, J.E., Gardner, R.H., Brenkert, A.L., 1986. Individual parameter perturbation and error analysis of fish bioenergetics models. Canadian Journal of Fisheries and Aquatic Sciences 43 (1), 160–168. https://doi.org/10.1139/f86-018.

Bernhardt, J.R., Sunday, J.M., Thompson, P.L., O'Connor, M.I., 2018. Nonlinear averaging of thermal experience predicts population growth rates in a thermally variable environment. Proceedings of the Royal Society B: Biological Sciences 285 (1886), 20181076.

Bi, H., Peterson, W.T., Strub, P.T., 2011. Transport and coastal zooplankton communities in the northern California Current system. Geophysical Research Letters 38 (12). https://doi.org/10.1029/2011GL047927.

Black, B.A., Schroeder, I.D., Sydeman, W.J., Bograd, S.J., Lawson, P.W., 2010. Wintertime ocean conditions synchronize rockfish growth and seabird reproduction in the central California Current ecosystem. Canadian Journal of Fisheries and Aquatic Sciences 67 (7), 1149–1158. https://doi.org/10.1139/F10-055.

Blaxter, J.T., 1969. 4 development: eggs and larvae. In: Fish physiology, 3. Academic Press, pp. 177–252. https://doi.org/10.1016/S1546-5098(08)60114-4.

Boehlert, G.W., 1978. Changes in the oxygen consumption of prejuvenile rockfish, Sebastes diploproa, prior to migration from the surface to deep water. Physiological Zoology 51 (1), 56–67.

Boehlert, G.W., 1981. The role of temperature and photoperiod on the ontogenic migration of pre-juvenile Sebastes diploproa. Calif. Fish Game 67, 164–175.

Boehlert, G.W., Yoklavich, M.M., 1983. Effects of temperature, ration, and fish size on growth of juvenile black rockfish, Sebastes melanops. Environmental Biology of Fishes 8, 17–28. https://doi.org/10.1007/BF00004942.

Bograd, S.J., Schroeder, I., Sarkar, N., Qiu, X., Sydeman, W.J., Schwing, F.B., 2009. Phenology of coastal upwelling in the California Current. Geophysical Research Letters 36 (1). https://doi.org/10.1029/2008GL035933.

Bosley, K.L., Miller, T.W., Brodeur, R.D., Bosley, K.M., Van Gaest, A., Elz, A., 2014. Feeding ecology of juvenile rockfishes off Oregon and Washington based on stomach content and stable isotope analyses. Marine biology 161, 2381–2393. https://doi.org/10.1007/s00227-014-2513-8.

Brandt, S.B., Mason, D.M., Patrick, E.V., 1992. Spatially-explicit models of fish growth rate. Fisheries 17 (2), 23–35. https://doi.org/10.1577/1548-8446(1992)017≤0023:SMOFGR≥2.0.CO;2.

Brodie, S., Taylor, M.D., Smith, J.A., Suthers, I.M., Gray, C.A., Payne, N.L., 2016. Improving consumption rate estimates by incorporating wild activity into a bioenergetics model. Ecology and Evolution 6 (8), 2262–2274. https://doi.org/10.1002/ece3.2027.

Brown, J.H., Gillooly, J.F., Allen, A.P., Savage, V.M., West, G.B., 2004. Toward a metabolic theory of ecology. Ecology 85 (7), 1771–1789. https://doi.org/10.1890/03-9000.

Caselle, J.E., Wilson, J.R., Carr, M.H., Malone, D.P., Wendt, D.E., 2010. Can we predict interannual and regional variation in delivery of pelagic juveniles to nearshore populations of rockfishes (Genus *Sebastes*) using simple proxies of ocean conditions? California Cooperative Oceanic Fisheries Investigations Reports 51, 91–105.

Caswell, H., 2001. Matrix population models, 1. Sinauer, Sunderland, MA.

Chavez, F.P., Messié, M., 2009. A comparison of eastern boundary upwelling ecosystems. Progress in Oceanography 83 (1-4), 80–96. https://doi.org/10.1016/j.pocean.2009.07.032.

Checkley Jr, D.M., Barth, J.A., 2009. Patterns and processes in the California Current System. Progress in Oceanography 83 (1-4), 49–64. https://doi.org/10.1016/j.pocean.2009.07.028.

Cheresh, J., Fiechter, J., 2020. Physical and biogeochemical drivers of alongshore pH and oxygen variability in the California Current System. Geophysical Research Letters 47 (19), e2020GL089553. https://doi.org/10.1029/2020GL089553.

Cheresh, J., Kroeker, K.J., Fiechter, J., 2023. Upwelling intensity and source water properties drive high interannual variability of corrosive events in the California Current. Scientific Reports 13 (1), 13013. https://doi.org/10.1038/s41598-023-39691-5.

Chipps, S.R., Wahl, D.H., 2008. Bioenergetics modeling in the 21st century: reviewing new insights and revisiting old constraints. Transactions of the American Fisheries Society 137 (1), 298–313. https://doi.org/10.1577/T05-236.1.

Crane, K.E., 2014. Environmental effects on growth of early life history stages of rockfishes (Sebastes) off Central California based on analysis of otolith growth patterns. Humboldt State University.

Cushing, D.H., 1969. The regularity of the spawning season of some fishes. ICES Journal of Marine Science 33 (1), 81–92. https://doi.org/10.1093/icesjms/33.1.81.

Cushing, D.H., 1982. Climate and Fisheries. Academic Press, London, p. 373. https://doi.org/10.1016/0025-326X(83)90049-8.

Cushing, D.H., 1990. Plankton production and year-class strength in fish populations: an update of the match/mismatch hypothesis. In: Advances in marine biology, 26. Academic Press, pp. 249–293. https://doi.org/10.1016/S0065-2881(08)60202-3.

Denny, M., 2019. Performance in a variable world: using Jensen's inequality to scale up from individuals to populations. Conservation Physiology 7 (1), coz053.

Deslauriers, D., Chipps, S.R., Breck, J.E., Rice, J.A., Madenjian, C.P., 2017. Fish bioenergetics 4.0: an R-based modeling application. Fisheries 42 (11), 586–596. https://doi.org/10.1080/03632415.2017.1377558.

Dick, E.J., 2004. Beyond 'lognormal versus gamma': discrimination among error distributions for generalized linear models. Fisheries Research 70 (2-3), 351–366. https://doi.org/10.1016/j.fishres.2004.08.013.

Dick, E.J., Beyer, S., Mangel, M., Ralston, S., 2017. A meta-analysis of fecundity in rockfishes (genus Sebastes). Fisheries Research 187, 73–85. https://doi.org/10.1016/j.fishres.2016.11.009.

Downie, A.T., Illing, B., Faria, A.M., Rummer, J.L., 2020. Swimming performance of marine fish larvae: review of a universal trait under ecological and environmental pressure. Reviews in Fish Biology and Fisheries 30, 93–108.

Durant, J.M., Hjermann, D.Ø., Anker-Nilssen, T., Beaugrand, G., Mysterud, A., Pettorelli, N., Stenseth, N.C., 2005. Timing and abundance as key mechanisms affecting trophic interactions in variable environments. Ecology Letters 8 (9), 952–958. https://doi.org/10.1111/j.1461-0248.2005.00798.x.

Durant, J.M., Hjermann, D.Ø., Ottersen, G., Stenseth, N.C., 2007. Climate and the match or mismatch between predator requirements and resource availability. Climate research 33 (3), 271–283. https://doi.org/10.3354/cr033271.

Durant, J.M., Hjermann, D.Ø., Falkenhaug, T., Gifford, D.J., Naustvoll, L.J., Sullivan, B. K., Beaugrand, G., Stenseth, N.C., 2013. Extension of the match-mismatch hypothesis to predator-controlled systems. Marine Ecology Progress Series 474, 43–52. https://doi.org/10.3354/meps10089.

Durant, J.M., Molinero, J.C., Ottersen, G., Reygondeau, G., Stige, L.C., Langangen, Ø., 2019. Contrasting effects of rising temperatures on trophic interactions in marine ecosystems. Scientific Reports 9 (1), 15213. https://doi.org/10.1038/s41598-019-51607-w.

Ellertsen, B., Fossum, P., Solemdal, P., Sundby, S., 1989. Relation between temperature and survival of eggs and first-feeding larvae of northeast Arctic cod (Gadus morhua L. Rapport et Proces-verbaux des Réunions du Conseil international pour l'Exploration de la Mer 191, 209–219.

Fennie, H.W., Grorud-Colvert, K., Sponaugle, S., 2023. Larval rockfish growth and survival in response to anomalous ocean conditions. Scientific Reports 13 (1), 4089. https://doi.org/10.1038/s41598-023-30726-5.

Fennie, H.W., Sponaugle, S., Daly, E.A., Brodeur, R.D., 2020. Prey tell: what quillback rockfish early life history traits reveal about their survival in encounters with juvenile coho salmon. Marine Ecology Progress Series 650, 7–18. https://doi.org/10.3354/meps13300.

Fiechter, J., Edwards, C.A., Moore, A.M., 2018. Wind, circulation, and topographic effects on alongshore phytoplankton variability in the California Current. Geophysical Research Letters 45 (7), 3238–3245. https://doi.org/10.1002/2017GL076839.

Fiechter, J., Santora, J.A., Chavez, F., Northcott, D., Messié, M., 2020. Krill hotspot formation and phenology in the California Current Ecosystem. Geophysical research letters 47 (13), e2020GL088039. https://doi.org/10.1029/2020GL088039.

Fiechter, J., Pozo Buil, M., Jacox, M.G., Alexander, M.A., Rose, K.A., 2021. Projected shifts in 21st century sardine distribution and catch in the California Current. Frontiers in Marine Science 874. https://doi.org/10.3389/fmars.2021.685241.

Field, J.C., Miller, R.R., Santora, J.A., Tolimieri, N., Haltuch, M.A., Brodeur, R.D., Auth, T.D., Dick, E.J., Monk, M.H., Sakuma, K.M., Wells, B.K., 2021. Spatiotemporal patterns of variability in the abundance and distribution of winter-spawned pelagic juvenile rockfish in the California Current. PloS one 16 (5), e0251638. https://doi.org/10.1371/journal.pone.0251638.

Friedman, W.R., Santora, J.A., Schroeder, I.D., Huff, D.D., Brodeur, R.D., Field, J.C., Wells, B.K., 2018. Environmental and geographic relationships among salmon forage assemblages along the continental shelf of the California Current. Marine Ecology Progress Series 596, 181–198. https://doi.org/10.3354/meps12598.

Fry, F.E.J., 1971. The effect of environmental factor on the physiology of fish. In: Hoar, W.S., Randell, D.J. (Eds.), Fish Physiology: Environment Relation and Behaviour. Academic Press, New York, pp. 1–98.

Giménez, L., 2011. Exploring mechanisms linking temperature increase and larval phenology: the importance of variance effects. Journal of Experimental Marine Biology and Ecology 400 (1-2), 227–235. https://doi.org/10.1016/j.jembe.2011.02.036.

Haidvogel, D.B., Arango, H., Budgell, W.P., Cornuelle, B.D., Curchitser, E., Di Lorenzo, E., Fennel, K., Geyer, W.R., Hermann, A.J., Lanerolle, L., Levin, J., 2008. Ocean forecasting in terrain-following coordinates: Formulation and skill assessment of the Regional Ocean Modeling System. Journal of computational physics 227 (7), 3595–3624. https://doi.org/10.1016/j.jcp.2007.06.016.

Hamilton, S.L., Logan, C.A., Fennie, H.W., Sogard, S.M., Barry, J.P., Makukhov, A.D., Tobosa, L.R., Boyer, K., Lovera, C.F., Bernardi, G., 2017. Species-specific responses of juvenile rockfish to elevated p CO2: from behavior to genomics. PLoS One 12 (1), e0169670. https://doi.org/10.1371/journal.pone.0169670.

Hanson, P.C., Johnson, T.B., Schindler, D.E., Kitchell, J.F., 1997. Technical Report WISCU-T-97-001. University of Wisconsin Sea Grant Institute, Madison, Wisconsin.

Hare, J.A., Cowen, R.K., 1995. Effect of age, growth rate, and ontogeny on the otolith size–fish size relationship in bluefish, Pomatomus saltatrix, and the implications for back-calculation of size in fish early life history stages. Canadian Journal of Fisheries and Aquatic Sciences 52 (9), 1909–1922. https://doi.org/10.1139/f95-783.

Hartman, K.J., Kitchell, J.F., 2008. Bioenergetics modeling: progress since the 1992 symposium. Transactions of the American Fisheries Society 137 (1), 216–223. https://doi.org/10.1577/T07-040.1.

Harvey, C.J., 2005. Effects of El Nino events on energy demand and egg production of rockfish (Scorpaenidae: Sebastes): a bioenergetics approach. Fishery Bulletin 103, 71–83.

Harvey, C.J., 2009. Effects of temperature change on demersal fishes in the California Current: a bioenergetics approach. Canadian Journal of Fisheries and Aquatic Sciences 66 (9), 1449–1461. https://doi.org/10.1139/F09-087.

Harvey, C.J., Field, J.C., Beyer, S.G., Sogard, S.M., 2011. Modeling growth and reproduction of chilipepper rockfish under variable environmental conditions. Fisheries Research 109 (1), 187–200. https://doi.org/10.1016/j.fishres.2011.02.004.

Hazen, E.L., Jorgensen, S., Rykaczewski, R.R., Bograd, S.J., Foley, D.G., Jonsen, I.D., Shaffer, S.A., Dunne, J.P., Costa, D.P., Crowder, L.B., Block, B.A., 2013. Predicted habitat shifts of Pacific top predators in a changing climate. Nature Climate Change 3 (3), 234–238. https://doi.org/10.1038/nclimate1686.

Henderson, M., Fiechter, J., Huff, D.D., Wells, B.K., 2019. Spatial variability in ocean-mediated growth potential is linked to Chinook salmon survival. Fisheries Oceanography 28 (3), 334–344. https://doi.org/10.1111/fog.12415.

Hewett, S.W., Johnson, B.L., 1987. Technical Report No. WIS-SG-87-245. University of Wisconsin Sea Grant Institute, Madison, WI.

Hewett, S.W., Johnson, B.L., 1992. Technical Report No. WIS-SG-91-250. University of Wisconsin Sea Grant Institute, Madison, WI.

Hixon, M.A., Johnson, D.W., Sogard, S.M., 2014. BOFFFFs: on the importance of conserving old growth age structure in fishery populations. ICES Journal of Marine Science 71 (8), 2171–2185. https://doi.org/10.1093/icesjms/fst200.

Hjort, J., 1914. Fluctuations in the great fisheries of northern Europe. Rapports Procès Verbaux des Réunions Conseil Permanent International l'Exploration Mer 20, 1.

Hollowed, A.B., Aydin, K.Y., Essington, T.E., Ianelli, J.N., Megrey, B.A., Punt, A.E., Smith, A.D., 2011. Experience with quantitative ecosystem assessment tools in the northeast Pacific. Fish and Fisheries 12 (2), 189–208. https://doi.org/10.1111/j.1467-2979.2011.00413.x.

Holsman, K., Danner, E., 2016. Numerical integration of temperature-dependent functions in bioenergetics models to avoid overestimation of fish growth. Transactions of the American Fisheries Society 145 (2), 334–347. https://doi.org/10.1080/00028487.2015.1094129.

Houde, E.D., 1987. Fish early life dynamics and recruitment variability. In Am. Fish. Soc. Symp. 2, 17–29.

Houde, E.D., 1989. Subtleties and episodes in the early life of fishes. Journal of Fish Biology 35, 29–38. https://doi.org/10.1111/j.1095-8649.1989.tb03043.x.

Houde, E.D., 1997. Patterns and consequences of selective processes in teleost early life histories. Early life history and recruitment in fish populations. Springer, DordrechtNetherlands, pp. 173–196.

Houde, E.D., 2008. Emerging from Hjort's shadow. Journal of Northwest Atlantic Fishery Science 41.

Houde, E.D., 2016. Recruitment variability. In: Jakobsen, T., Fogarty, M., Megrey, B., Moksness, E. (Eds.), Reproductive Biology of Fishes: Implications for Assessment and Management, 2nd Edn. John Wiley & Sons, Ltd, Hoboken, NJ, pp. 98–187. https://doi.org/10.1002/9781118752739.ch3.

Ito, S.I., Kishi, M.J., Kurita, Y., Oozeki, Y., Yamanaka, Y., Megrey, B.A., Werner, F.E., 2004. Initial design for a fish bioenergetics model of Pacific saury coupled to a lower trophic ecosystem model. Fisheries Oceanography 13, 111–124. https://doi.org/10.1111/j.1365-2419.2004.00307.x.

Jahncke, J., Saenz, B.L., Abraham, C.L., Rintoul, C., Bradley, R.W., Sydeman, W.J., 2008. Ecosystem responses to short-term climate variability in the Gulf of the Farallones, California. Progress in Oceanography 77 (2–3), 182–193.

Jensen, J.L.W.V., 1906. Sur les fonctions convexes et les inégalités entre les valeurs moyennes. Acta Mathematica 30 (1), 175–193.

Ji, R., Edwards, M., Mackas, D.L., Runge, J.A., Thomas, A.C., 2010. Marine plankton phenology and life history in a changing climate: current research and future directions. Journal of plankton research 32 (10), 1355–1368. https://doi.org/10.1093/plankt/fbq062.

Johnson, K.A., Yoklavich, M.M., Cailliet, G.M., 2001. California Cooperative Oceanic Fisheries Investigations Report, pp. 153–166.

Jørgensen, C., Enberg, K., Mangel, M., 2016. Modelling and interpreting fish bioenergetics: a role for behaviour, life-history traits and survival trade-offs. Journal of fish biology 88 (1), 389–402. https://doi.org/10.1111/jfb.12834.

Kashef, N.S., Sogard, S.M., Fisher, R., Largier, J.L., 2014. Ontogeny of critical swimming speeds for larval and pelagic juvenile rockfishes (Sebastes spp., family Scorpaenidae). Marine Ecology Progress Series 500, 231–243. https://doi.org/10.3354/meps10669.

Kishi, M.J., Kashiwai, M., Ware, D.M., Megrey, B.A., Eslinger, D.L., Werner, F.E., Noguchi-Aita, M., Azumaya, T., Fujii, M., Hashimoto, S., Huang, D., 2007. NEMURO—a lower trophic level model for the North Pacific marine ecosystem. Ecological Modelling 202 (1-2), 12–25. https://doi.org/10.1016/j.ecolmodel.2006.08.021.

Kitchell, J.F., Stewart, D.J., Weininger, D., 1977. Applications of a bioenergetics model to yellow perch (Perca flavescens) and walleye (Stizostedion vitreum vitreum). Journal of the Fisheries Board of Canada 34 (10), 1922–1935. https://doi.org/10.1139/f77-258.

Koenigstein, S., Jacox, M.G., Pozo Buil, M., Fiechter, J., Muhling, B.A., Brodie, S., Kuriyama, P.T., Auth, T.D., Hazen, E.L., Bograd, S.J., Tommasi, D., 2022. Population projections of Pacific sardine driven by ocean warming and changing food availability in the California Current. ICES Journal of Marine Science 79 (9), 2510–2523. https://doi.org/10.1093/icesjms/fsac191.

Kooijman, B., Kooijman, S.A.L.M., 2010. Dynamic energy budget theory for metabolic organisation, 3rd Ed. Cambridge University Press. https://doi.org/10.1017/CBO9780511805400.

Laidig, T.E., Ralston, S., Bence, J.R., 1991. Dynamics of growth in the early life history of shortbelly rockfish Sebastes jordani. Fish. Bull. 89, 611–621.

Laidig, T.E., 2010. Influence of ocean conditions on the timing of early life history events for blue rockfish (Sebastes mystinus) off California 108, 442–449.

Laidig, T.E., Chess, J.R., Howard, D.F., 2007. Relationship between abundance of juvenile rockfishes (Sebastes spp.) and environmental variables documented off

northern California and potential mechanisms for the covariation. Fishery Bulletin 105 (1), 39–49.
Larson, R.J., Lenarz, W.H., Ralston, S.T.E.P.H.E.N., 1994. The distribution of pelagic juvenile rockfish of the genus Sebastes in the upwelling region off central California. Calif. Coop. Ocean. Fish. Investig. Rep 35, 175–221.
Leis, J.M., 2007. Behaviour as input for modelling dispersal of fish larvae: behaviour, biogeography, hydrodynamics, ontogeny, physiology and phylogeny meet hydrography. Marine Ecology Progress Series 347, 185–193. https://doi.org/10.3354/meps06977.
Lenarz, W.H., Ventresca, D.A., Graham, W.M., Schwing, F.B., Chavez, F.P., 1995. Explorations of El Niño events and associated biological population dynamics off central California. California Cooperative Oceanic Fisheries Investigations Report 36, 106–119.
Love, M.S., Yoklavich, M., Thorsteinson, L.K., 2002. The rockfishes of the northeast Pacific. Univ of California Press, Los Angeles, p. 414.
MacFarlane, R.B., Norton, E.C., 1999. Nutritional dynamics during embryonic development in the viviparous genus Sebastes and their application to the assessment of reproductive success. Fish. Bull. 97, 273–281.
Maunder, M.N., Punt, A.E., 2004. Standardizing catch and effort data: a review of recent approaches. Fisheries research 70 (2-3), 141–159. https://doi.org/10.1016/j.fishres.2004.08.002.
McGowan, J.A., Cayan, D.R., Dorman, L.M., 1998. Climate-ocean variability and ecosystem response in the Northeast Pacific. Science 281 (5374), 210–217. https://doi.org/10.1126/science.281.5374.210.
Megrey, B.A., Rose, K.A., Klumb, R.A., Hay, D.E., Werner, F.E., Eslinger, D.L., Smith, S.L., 2007. A bioenergetics-based population dynamics model of Pacific herring (Clupea harengus pallasi) coupled to a lower trophic level nutrient–phytoplankton–zooplankton model: description, calibration, and sensitivity analysis. Ecological modelling 202 (1-2), 144–164. https://doi.org/10.1016/j.ecolmodel.2006.08.020.
Miller, T.J., Crowder, L.B., Rice, J.A., Marschall, E.A., 1988. Larval size and recruitment mechanisms in fishes: toward a conceptual framework. Canadian Journal of Fisheries and Aquatic Sciences 45 (9), 1657–1670. https://doi.org/10.1139/f88-197.
Miller, T.W., Brodeur, R.D., 2007. Diet of and trophic relationships among dominant marine nekton within the Northern California Current ecosystem. Fish Bull 105, 548–559.
Miller, T.W., Brodeur, R.D., Rau, G., Omori, K., 2010. Prey dominance shapes trophic structure of the northern California Current pelagic food web: evidence from stable isotopes and diet analysis. Marine Ecology Progress Series 420, 15–26. https://doi.org/10.3354/meps08876.
Moser, H.G., Boehlert, G.W., 1991. Ecology of pelagic larvae and juveniles of the genus Sebastes. Environmental Biology of Fishes 30, 203–224. https://doi.org/10.1007/BF02296890.
Mulder, C., Hendriks, A.J., 2014. Half-saturation constants in functional responses. Global Ecology and Conservation 2, 161–169. https://doi.org/10.1016/j.gecco.2014.09.006.
Munday, P.L., Leis, J.M., Lough, J.M., Paris, C.B., Kingsford, M.J., Berumen, M.L., Lambrechts, J., 2009. Climate change and coral reef connectivity. Coral reefs 28, 379–395. https://doi.org/10.1007/s00338-008-0461-9.
Norton, E.C., MacFarlane, R.B., Mohr, M.S., 2001. Lipid class dynamics during development in early life stages of shortbelly rockfish and their application to condition assessment. Journal of Fish Biology 58 (4), 1010–1024. https://doi.org/10.1111/j.1095-8649.2001.tb00551.x.
O'Connor, M.I., Bruno, J.F., Gaines, S.D., Halpern, B.S., Lester, S.E., Kinlan, B.P., Weiss, J.M., 2007. Temperature control of larval dispersal and the implications for marine ecology, evolution, and conservation. Proceedings of the National Academy of Sciences 104 (4), 1266–1271. https://doi.org/10.1073/pnas.0603422104.
Peck, M.A., Hufnagl, M., 2012. Can IBMs tell us why most larvae die in the sea? Model sensitivities and scenarios reveal research needs. Journal of Marine Systems 93, 77–93. https://doi.org/10.1016/j.jmarsys.2011.08.005.
Peck, M.A., Moyano, M., 2016. Measuring respiration rates in marine fish larvae: challenges and advances. Journal of Fish Biology 88 (1), 173–205. https://doi.org/10.1111/jfb.12810.
Pepin, P., 1991. Effect of temperature and size on development, mortality, and survival rates of the pelagic early life history stages of marine fish. Canadian Journal of Fisheries and Aquatic Sciences 48 (3), 503–518. https://doi.org/10.1139/f91-06.
Peterson, W.T., Fisher, J.L., Peterson, J.O., Morgan, C.A., Burke, B.J., Fresh, K.L., 2014. Applied fisheries oceanography: Ecosystem indicators of ocean conditions inform fisheries management in the California Current. Oceanography 27 (4), 80–89. https://doi.org/10.5670/oceanog.2014.88.
Pörtner, H.O., Farrell, A.P., 2008. Physiology and climate change. Science 322 (5902), 690–692. https://doi.org/10.1126/science.1163156.
Pörtner, H.O., Knust, R., 2007. Climate change affects marine fishes through the oxygen limitation of thermal tolerance. science 315 (5808), 95–97. https://doi.org/10.1126/science.1135471.
Pozo Buil, M., Jacox, M.G., Fiechter, J., Alexander, M.A., Bograd, S.J., Curchitser, E.N., Edwards, C.A., Rykaczewski, R.R., Stock, C.A., 2021. A dynamically downscaled ensemble of future projections for the California current system. Frontiers in Marine Science 8, 612874. https://doi.org/10.3389/fmars.2021.612874.
Ralston, S., Howard, D.F., 1995. On the development of year-class strength and cohort variability in two northern California rockfishes. Fish. Bull. 93, 710–720.
Ralston, S., Stewart, I.J., 2013. Anomalous distributions of pelagic juvenile rockfish on the US west coast in 2005 and 2006. California Cooperative Oceanic and Fisheries Investigations Reports 54, 155–166.
Ralston, S., Bence, J.R., Eldridge, M.B., Lenarz, W.H., 2003. An approach to estimating rockfish biomass based on larval production, with application to *Sebastes jordani*. Fishery Bulletin 101, 129–146.
Ralston, S., Sakuma, K.M., Field, J.C., 2013. Interannual variation in pelagic juvenile rockfish (Sebastes spp.) abundance–going with the flow. Fisheries Oceanography 22 (4), 288–308. https://doi.org/10.1111/fog.12022.
Rebstock, G.A., 2001. Long-term stability of species composition in calanoid copepods off southern California. Marine Ecology Progress Series 215, 213–224. https://doi.org/10.3354/meps215213.
Reilly, C.A., Echeverria, T.W., Ralston, S., 1992. Interannual variation and overlap in the diets of pelagic juvenile rockfish(genus: Sebastes) off Central California. Fishery Bulletin 90 (3), 505–515.
Ricker, W.E., 1979. Growth rates and models. Fish physiology 677–744.
Robert, D., Shoji, J., Sirois, P., Takasuka, A., Catalán, I.A., Folkvord, A., Ludsin, S.A., Peck, M.A., Sponaugle, S., Ayón, P.M., Brodeur, R.D., 2023. Life in the fast lane: Revisiting the fast growth—High survival paradigm during the early life stages of fishes. Fish and Fisheries 24 (5), 863–888. https://doi.org/10.1111/faf.12774.
Rooper, C.N., Boldt, J.L., Batten, S., Gburski, C., 2012. Growth and production of Pacific ocean perch (Sebastes alutus) in nursery habitats of the Gulf of Alaska. Fisheries Oceanography 21 (6), 415–429. https://doi.org/10.1111/j.1365-2419.2012.00635.x.
Rose, K.A., Rutherford, E.S., McDermot, D.S., Forney, J.L., Mills, E.L., 1999(a). Individual-based model of yellow perch and walleye populations in Oneida Lake. Ecological Monographs 69 (2), 127–154. https://doi.org/10.1890/0012-9615(1999)069[0127:IBMOYP]2.0.CO;2.
Rose, K.A., Cowan Jr, J.H., Clark, M.E., Houde, E.D., Wang, S.B., 1999(b). An individual-based model of bay anchovy population dynamics in the mesohaline region of Chesapeake Bay. Marine Ecology Progress Series 185, 113–132. https://doi.org/10.3354/meps185113.
Rose, K.A., Fiechter, J., Curchitser, E.N., Hedstrom, K., Bernal, M., Creekmore, S., Haynie, A., Ito, S.I., Lluch-Cota, S., Megrey, B.A., Edwards, C.A., 2015. Demonstration of a fully-coupled end-to-end model for small pelagic fish using sardine and anchovy in the California Current. Progress in Oceanography, 138, 348–380. https://doi.org/10.1016/j.pocean.2015.01.012.
Ross, J.R., Larson, R.J., 2003. Influence of water column stratification on the depth distributions of pelagic juvenile rockfishes off central California. California Cooperative Oceanic Fisheries Investigations Reports 44, 65–75.
Ruel, J.J., Ayres, M.P., 1999. Jensen's inequality predicts effects of environmental variation. Trends in Ecology & Evolution 14 (9), 361–366.
Sakuma, K.M., Field, J.C., Mantua, N.J., Ralston, S., Marinovic, B.B., Carrion, C.N., 2016. Anomalous epipelagic micronekton assemblage patterns in the neritic waters of the California Current in spring 2015 during a period of extreme ocean conditions. California Cooperative Oceanic Fisheries Investigations Report 57, 163–183.
Santora, J.A., Schroeder, I.D., Field, J.C., Wells, B.K., Sydeman, W.J., 2014. Spatio-temporal dynamics of ocean conditions and forage taxa reveal regional structuring of seabird–prey relationships. Ecological Applications 24 (7), 1730–1747. https://doi.org/10.1002/2014GL061045.
Santora, J.A., Hazen, E.L., Schroeder, I.D., Bograd, S.J., Sakuma, K.M., Field, J.C., 2017. Impacts of ocean climate variability on biodiversity of pelagic forage species in an upwelling ecosystem. Marine Ecology Progress Series 580, 205–220. https://doi.org/10.3354/meps12278.
Schroeder, I.D., Sydeman, W.J., Sarkar, N., Thompson, S.A., Bograd, S.J., Schwing, F.B., 2009. Winter pre-conditioning of seabird phenology in the California Current. Marine Ecology Progress Series 393, 211–223. https://doi.org/10.3354/meps08103.
Schroeder, I.D., Black, B.A., Sydeman, W.J., Bograd, S.J., Hazen, E.L., Santora, J.A., Wells, B.K., 2013. The North Pacific High and wintertime pre-conditioning of California current productivity. Geophysical Research Letters 40 (3), 541–546. https://doi.org/10.1002/grl.50100.
Schroeder, I.D., Santora, J.A., Moore, A.M., Edwards, C.A., Fiechter, J., Hazen, E.L., Bograd, S.J., Field, J.C., Wells, B.K., 2014. Application of a data-assimilative regional ocean modeling system for assessing California Current System ocean conditions, krill, and juvenile rockfish interannual variability. Geophysical Research Letters 41 (16), 5942–5950. https://doi.org/10.1002/2014GL061045.
Schroeder, I.D., Santora, J.A., Bograd, S.J., Hazen, E.L., Sakuma, K.M., Moore, A.M., Edwards, C.A., Wells, B.K., Field, J.C., 2019. Source water variability as a driver of rockfish recruitment in the California Current Ecosystem: implications for climate change and fisheries management. Canadian Journal of Fisheries and Aquatic Sciences 76 (6), 950–960. https://doi.org/10.1139/cjfas-2017-0480.
Schwing, F.B., Bond, N.A., Bograd, S.J., Mitchell, T., Alexander, M.A., Mantua, N., 2006. Delayed coastal upwelling along the US West Coast in 2005: A historical perspective. Geophysical Research Letters 33 (22). https://doi.org/10.1029/2006GL026911.
Shaffer, J.A., Doty, D.C., Buckley, R.M., West, J.E., 1995. Crustacean community composition and trophic use of the drift vegetation habitat by juvenile splitnose rockfish *Sebastes diploproa*. Marine Ecology Progress Series 123, 13–21. https://doi.org/10.3354/meps123013.
Shchepetkin, A.F., McWilliams, J.C., 2005. The regional oceanic modeling system (ROMS): a split-explicit, free-surface, topography-following-coordinate oceanic model. Ocean modelling 9 (4), 347–404. https://doi.org/10.1016/j.ocemod.2004.08.002.
Sibly, R.M., Grimm, V., Martin, B.T., Johnston, A.S., Kułakowska, K., Topping, C.J., Calow, P., Nabe-Nielsen, J., Thorbek, P., DeAngelis, D.L., 2013. Representing the acquisition and use of energy by individuals in agent-based models of animal populations. Methods in Ecology and Evolution 4 (2), 151–161. https://doi.org/10.1111/2041-210x.12002.
Sinclair, M., 1988. Marine populations. An essay on population regulation and speciation. Washington Sea Grant, Seattle, WAUSA.

Sogard, S.M., 1997. Size-selective mortality in the juvenile stage of teleost fishes: a review. Bulletin of marine science 60 (3), 1129–1157.

Stefánsson, G., 1996. Analysis of groundfish survey abundance data: combining the GLM and delta approaches. ICES journal of Marine Science 53 (3), 577–588. https://doi.org/10.1006/jmsc.1996.0079.

Stevenson, D.K., Campana, S.E., 1992. Otolith Microstructure Examination and Analysis. Department of Fisheries and Oceans, Ottawa, Canada.

Sumida, B.Y., Moser, H.G., 1984. Food and feeding of bocaccio (*Sebastes paucispinis*) and comparison with Pacific hake (*Merluccius productus*) larvae in the California Current. Calif. Coop. Oceanic Fish. Invest. Rep. 25, 112–118.

Sydeman, W.J., Bradley, R.W., Warzybok, P., Abraham, C.L., Jahncke, J., Hyrenbach, K. D., Kousky, V., Hipfner, J.M., Ohman, M.D., 2006. Planktivorous auklet Ptychoramphus aleuticus responses to ocean climate, 2005: Unusual atmospheric blocking? Geophysical Research Letters 33 (22). https://doi.org/10.1029/2006GL026736.

Szoboszlai, A.I., Thayer, J.A., Wood, S.A., Sydeman, W.J., Koehn, L.E., 2015. Forage species in predator diets: synthesis of data from the California Current. Ecological Informatics 29, 45–56. https://doi.org/10.1016/j.ecoinf.2015.07.003.

Thomas, A.C., Brickley, P., 2006. Satellite measurements of chlorophyll distribution during spring 2005 in the California Current. Geophysical Research Letters 33 (22). https://doi.org/10.1029/2006GL026588.

Thompson, A.R., Hyde, J.R., Watson, W., Chen, D.C., Guo, L.W., 2016. Rockfish assemblage structure and spawning locations in southern California identified through larval sampling. Marine Ecology Progress Series 547, 177–192. https://doi.org/10.3354/meps11633.

Thompson, A.R., Chen, D.C., Guo, L.W., Hyde, J.R., Watson, W., 2017. Larval abundances of rockfishes that were historically targeted by fishing increased over 16 years in association with a large marine protected area. Royal Society open science 4 (9), 170639. https://doi.org/10.1098/rsos.170639.

Thornton, K.W., Lessem, A.S., 1978. A temperature algorithm for modifying biological rates. Transactions of the American Fisheries Society 107 (2), 284–287. https://doi.org/10.1577/1548-8659(1978)107≤284:ATAFMB≥2.0.CO;2.

Wells, B.K., Santora, J.A., Henderson, M.J., Warzybok, P., Jahncke, J., Bradley, R.W., Huff, D.D., Schroeder, I.D., Nelson, P., Field, J.C., Ainley, D.G., 2017. Environmental conditions and prey-switching by a seabird predator impact juvenile salmon survival. Journal of Marine Systems 174, 54–63. https://doi.org/10.1016/j.jmarsys.2017.05.008.

Wheeler, S.G., Anderson, T.W., Bell, T.W., Morgan, S.G., Hobbs, J.A., 2017. Regional productivity predicts individual growth and recruitment of rockfishes in a northern California upwelling system. Limnology and Oceanography 62 (2), 754–767. https://doi.org/10.1002/lno.10458.

Winberg, G.G., 1956. Rate of metabolism and food requirements of fishes. Fish. Res. Bd. Canada Trans. Ser. 433, 1–251. https://doi.org/10.2307/1440948.

Woodbury, D., Ralston, S., 1991. Interannual variation in growth rates and back-calculated birthdate distributions of pelagic juvenile rockfishes (Sebastes spp.) off the central California coast. Fish. Bull. 89, 523–533.

Wyllie-Echeverria, T.W., 1987. Thirty-four species of California rockfishes: maturity and seasonality of reproduction. Fishery Bulletin 85 (2), 229–250.

Yang, T.H., 1992. Doctoral dissertation. University of California, San Diego.

Young, K.V., Dower, J.F., Pepin, P., 2009. A hierarchical analysis of the spatial distribution of larval fish prey. Journal of Plankton Research 31 (6), 687–700. https://doi.org/10.1093/plankt/fbp017.